Chen *et al. Chem. Synth.* **2025**, *5*, 33
DOI: 10.20517/cs.2024.25

Chemical Synthesis

Mini Review

Open Access

Check for updates

Recent advances in bimetallic small-pore zeolite catalysts for ammonia-assisted selective catalytic reduction of NO_x

Mengyang Chen*, **Shi-Bin Ren, De-Man Han**

School of Pharmaceutical and Chemical Engineering, Taizhou University, Taizhou 318000, Zhejiang, China.

***Correspondence to:** Dr. Mengyang Chen, School of Pharmaceutical and Chemical Engineering, Taizhou University, No.1139 Shifu Avenue, Jiaojiang District, Taizhou 318000, Zhejiang, China. E-mail: mychen@tzc.edu.cn

How to cite this article: Chen, M.; Ren, S. B.; Han, D. M. Recent advances in bimetallic small-pore zeolite catalysts for ammonia-assisted selective catalytic reduction of NO_x. *Chem. Synth.* **2025**, *5*, 33. https://dx.doi.org/10.20517/cs.2024.25

Received: 27 Feb 2024 **First Decision:** 27 Jun 2024 **Revised:** 10 Jul 2024 **Accepted:** 2 Aug 2024 **Published:** 10 Mar 2025

Academic Editor: Yi Tang **Copy Editor:** Pei-Yun Wang **Production Editor:** Pei-Yun Wang

Abstract

Bimetallic small-pore zeolites containing Cu ions and secondary metal ions present a potential application value for ammonia-assisted selective catalytic reduction of nitrogen oxides (NO_x), showing superior catalytic activity and excellent hydrothermal stability compared to monometallic Cu-zeolites. The idea of introducing secondary metal ions aims to modulate the properties of Cu active sites. This review first summarizes the strategies of incorporating secondary metal ions into zeolites. Then, we delve into the impacts of varying loadings of secondary metal ions on the catalytic performance of zeolites. Finally, we emphasize the synergistic interactions between secondary metal ions and active Cu sites, focusing on their effects on the distribution, stability, and activity of the Cu active sites, which are adjusted by the presence of secondary metal ions. In conclusion, we wrap up this review and provide perspectives on the design and in-depth study on metal ions-doped Cu-zeolite catalysts.

Keywords: Zeolite, small pores, Cu-SSZ-13, NH_3-SCR reaction, bimetallic ions, Cu active sites

INTRODUCTION

Background

With the increasing global awareness of environmental issues, worldwide emission regulations have become increasingly stringent[1]. Nitrogen oxides (NO_x), which originate from transportation and industrial activities, can contribute to haze, photochemical smog and acid rain, posing a significant threat to human

health[2-4]. Among automobile exhaust emissions, NO_x emitted by diesel vehicles is the main source[4-6]. Furthermore, diesel engines are the primary power source for non-road mobile vehicles such as farming machinery and marine engines[4]. Their contribution of NO_x emission is comparable to that of road automobiles. Therefore, it is urgent to control the NO_x emission from diesel engines. Three-way catalysts (TWCs) containing noble metal-doped oxides were proposed as a means to eliminate NO_x[7]. However, TWCs have difficulty reducing NO_x in practical aftertreatment systems because of lean combustion conditions in diesel engines. Ammonia-assisted selective catalytic reduction (NH_3-SCR) technology has been effectively and commercially implemented for controlling diesel vehicle exhaust. This technology is known for its high efficiency in reducing NO_x emission and minimal secondary pollution emission under excess oxygen conditions[8-10].

Catalysts are indispensable in the NH_3-SCR reaction and have garnered considerable attention. Currently, vanadium (V)-based oxide catalysts are utilized in SCR systems[11-13]. However, the limited temperature range, inadequate hydrothermal stability, and elevated toxicity of V impede the further application of V-based oxide catalysts[14-16]. Transition metals and their oxides have been explored as viable alternatives to replace V-based catalysts. Manganese (Mn)-based oxide catalysts, extensively investigated, exhibit commendable low-temperature SCR activity[17]. Nevertheless, the presence of sulfur dioxide in the feed can easily deactivate Mn-based catalysts at low temperatures[18]. Furthermore, the hydrothermal stability of these catalysts necessitates further enhancement due to the presence of water vapor during the reaction and aging processes[19]. Hence, there is an instant imperative to construct NH_3-SCR catalysts that exhibit exceptional efficiency, superior hydrothermal stability, and a broad operating temperature range.

In the past few decades, zeolite-based catalysts have emerged as effective and versatile materials for various environmental applications[8]. Zeolites can be classified into different types based on their pore sizes, which include small-pore zeolites with eight-membered rings (8MRs), medium-pore zeolites with 10MRs, large-pore zeolites with 12MRs, and ultra-large-pore zeolites with pore sizes exceeding 12MRs. The diverse pore sizes enable zeolites to exhibit exceptional shape selectivity. Moreover, zeolites exhibit remarkable hydrothermal stability due to their highly crystalline framework structure, surpassing that of organic network materials such as covalent organic frameworks (COFs), covalent organic polymers (COPs), and metal-organic frameworks (MOFs). Additionally, abundant acid sites and ion-exchange sites endow the zeolites with the capacity to satisfy various chemical reactions. These inherent advantages make zeolites highly promising for applications in adsorption and separation, catalysis, luminescence, sensing, and electrochemistry[20-25]. The current study specifically focuses on exploring the application of zeolites in NH_3-SCR catalysis.

Copper-exchanged ZSM-5 zeolites (Cu-ZSM-5, medium pore, **MFI** topology) were first applied to reduce NO_x emission through direct decomposition of nitric oxide (NO) to N_2[26]. However, their low efficiency in removing NO_x did not meet practical application requirements, which prompts the emergence of zeolite-based NH_3-SCR technology[27-31]. In the aftertreatment system, the SCR unit is exposed to the high-temperature environment (above 650 °C) due to the regeneration of the upstream diesel particulate filter (DPF), necessitating SCR catalysts with excellent hydrothermal stability[4,32]. Besides, because of the complicated operating conditions in diesel engines, SCR catalysts must exhibit high catalytic activity across a broad temperature range of 200-600 °C, and maintain effectiveness at low temperatures (< 200 °C) during cold-start conditions[4,33,34]. Furthermore, catalyst poisoning is an unavoidable issue stemming from the incomplete oxidation of hydrocarbons (HCs) and CO, as well as the presence of sulfur-containing diesel fuel and alkali-metal-containing lubricating oil[35-37]. Therefore, SCR catalysts should possess the ability to cope with difficulties posed by the actual operating conditions.

The limited catalytic performance of metal-exchanged ZSM-5 zeolites has impeded their widespread application on a larger scale. Subsequent studies on beta (large pore, **BEA*** topology) zeolites also fail to overcome the challenge of the high-temperature operating conditions[38-40]. Fortunately, Cu ions-exchanged small-pore zeolites such as **CHA**, **LTA**, **KFI** and **AEI** topologies have been reported to show exceptional durability[41-51]. Mechanism studies show that the hydrolysis of framework aluminum (Al) and the aggregation of CuO_x from Cu^{2+} active sites are the two vital factors determining the hydrothermal stability of zeolites[4]. These processes are key contributors to the degradation or preservation of the zeolite structure under high-temperature and humid conditions. Understanding and controlling these factors are essential for enhancing the hydrothermal stability of zeolite catalysts in various applications. Moreover, intrinsic narrow pores (~3.8 Å) in small-pore zeolites can block the diffusion of larger detached Al species caused by dealumination during high-temperature hydrothermal aging treatment[52]. As a result, these detached Al species will reattach back into the zeolite framework as the zeolite undergoes colling. This phenomenon is the main contributing factor to the superior hydrothermal stability observed in small-pore zeolites.

Cu-SSZ-13 zeolites with **CHA** topology have been extensively studied, revealing the presence of Z_2Cu^{2+} and $[ZCu(OH)]^+$ (where Z stands for a negative charge) active sites[53-56]. The first site is located near the 6MR to balance paired negative charges. The second site is situated adjacent to the 8MR and is associated with a single negative charge. The distribution of these Cu active sites can be modified by tuning the Si/Al and Cu/Al ratios[57-59]. By controlling these ratios, it is possible to customize the relative abundance of two Cu active sites, thereby influencing the catalytic performance of Cu-SSZ-13 zeolites. Increasing Al content can generate more paired Al, resulting in more Z_2Cu^{2+}. In contrast, a high Cu content with a fixed Si/Al ratio contributes to an increased amount of $[ZCu(OH)]^+$. Moreover, the Al distribution with various paired Al content can be adjusted using different structure-directing agents (SDAs)[60-62].

In addition to adjusting the elemental compositions of intrinsic zeolites, introducing secondary metal ions into small-pore Cu-zeolites has been demonstrated as a facile strategy to enhance catalytic performance by regulating the acidity of zeolites and the properties of Cu active sites[63-67]. For instance, Gao *et al.* demonstrated that incorporating alkali metals into Cu-SSZ-13 helped relieve zeolite hydrolysis during hydrothermal aging by removing a portion of Brønsted acid sites, favoring enhanced hydrothermal stability of Cu-SSZ-13 zeolites[63]. Moreover, Usui *et al.* reported that doping Ce ions into Cu-SSZ-13 could stabilize the framework and thus led to the enhancement of hydrothermal stability[64]. Furthermore, incorporating Sm ions into Cu-SSZ-13 allowed for regulating Cu active sites to increase $[ZCu(OH)]^+$ content and boost the activity and stability of $[ZCu(OH)]^+$, thereby promoting overall catalytic performance of zeolite[65]. These examples confirm that incorporating secondary metal ions into small-pore Cu-zeolites has a virtual effect on both catalytic activity and hydrothermal stability of the zeolites.

In this review, we will begin by examining the strategies employed for the synthesis and preparation of bimetallic small-pore zeolites. Then, the content of secondary metal ions to the catalytic performance of zeolites will be discussed, followed by an exploration of the synergistic interactions between secondary metal ions containing alkali metal ions, transition metal ions, and rare earth metal ions and Cu ions. We will summarize the results of recent research on bimetallic small-pore zeolites. To conclude, we will present the challenges and prospects for the future design of small-pore Cu-zeolite catalysts doped with secondary metal ions.

NH_3-SCR reaction features

The NH_3-SCR reaction involves a multi-step process over a redox site in the catalyst. Because the NO_x composition contains NO and nitrogen dioxide (NO_2), the processes of the NH_3-SCR reaction can be

divided into three schemes. The "standard SCR" reaction occurs when only NO and NH_3 are present in the presence of oxygen, requiring the transfer of $12e^-$, which is expressed as[68-71]:

$$4NO + 4NH_3 + O_2 \rightarrow 4N_2 + 6H_2O \quad (1)$$

As the concentration of NO_2 in the reaction atmosphere increases, resulting from the partial oxidation of NO in the upstream diesel oxidation catalyst (DOC) unit in the aftertreatment system, a "fast SCR" reaction begins to proceed involving the equimolar amounts of NO and NO_2 with NH_3, which is written as[68-72]:

$$NO + NO_2 + 2NH_3 \rightarrow 2N_2 + 3H_2O \quad (2)$$

This reaction shows higher NO_x conversion efficiency with the transfer of $6e^-$ compared to "standard SCR"[73]. Further increasing NO_2 content can result in the occurrence of "NO_2-SCR" given in[68-72]:

$$6NO_2 + 8NH_3 \rightarrow 7N_2 + 12H_2O \quad (3)$$

Besides the three main reactions, several side reactions can compete with the main SCR reactions, affecting the overall performance of the catalyst in terms of NO_x conversion efficiency and N_2 selectivity. These reactions are listed below[70,71,74,75]:

$$4NH_3 + 3O_2 \rightarrow 2N_2 + 6H_2O \quad (4)$$

$$2NH_3 + 2O_2 \rightarrow N_2O + 3H_2O \quad (5)$$

$$4NH_3 + 4NO + 3O_2 \rightarrow 4N_2O + 6H_2O \quad (6)$$

$$2NH_3 + 2NO_2 \rightarrow N_2 + N_2O + 3H_2O \quad (7)$$

Despite the presence of an upstream DOC unit, NO is more abundant in diesel engine exhaust compared to NO_2. In addition, both "fast SCR" and "standard SCR" positively contribute to the reduction of NO_x emission. Although "NO_2-SCR" shows the slowest NO_x removal efficiency, it can probably lead to the formation of undesired N_2O that is regarded as a greenhouse gas.

MULTI-METALLIC SMALL-PORE ZEOLITES FOR NH_3-SCR REACTION

The strategies of preparing bimetallic small-pore zeolites

The incorporation of metal ions into zeolites is commonly achieved through various strategies, including impregnation, ion exchange (which includes solid ion exchange and solution ion exchange), and one-pot synthesis[76-79]. As illustrated in Figure 1, when preparing bimetallic small-pore zeolites using an impregnation or ion exchange method, Cu ions are usually preferentially introduced into the zeolite, followed by secondary metal ions. Compared to bimetallic zeolites prepared by the ion exchange strategy, the impregnation method often causes the aggregation of metal ions within the zeolite support, leading to the generation of large particles. In addition, the ion-exchange sequence can affect the forms of metals in zeolites[65,80,81]. In the case of the one-pot method, metal-organic complexes are often used as template agents to synthesize zeolites while simultaneously introducing metal ions. Yet, this approach often results in the aggregation of metal ions due to the high metal ions content in the synthetic system. For example, Ren *et al.* reported an alternative strategy for synthesizing Cu-SSZ-13 utilizing a novel template copper-

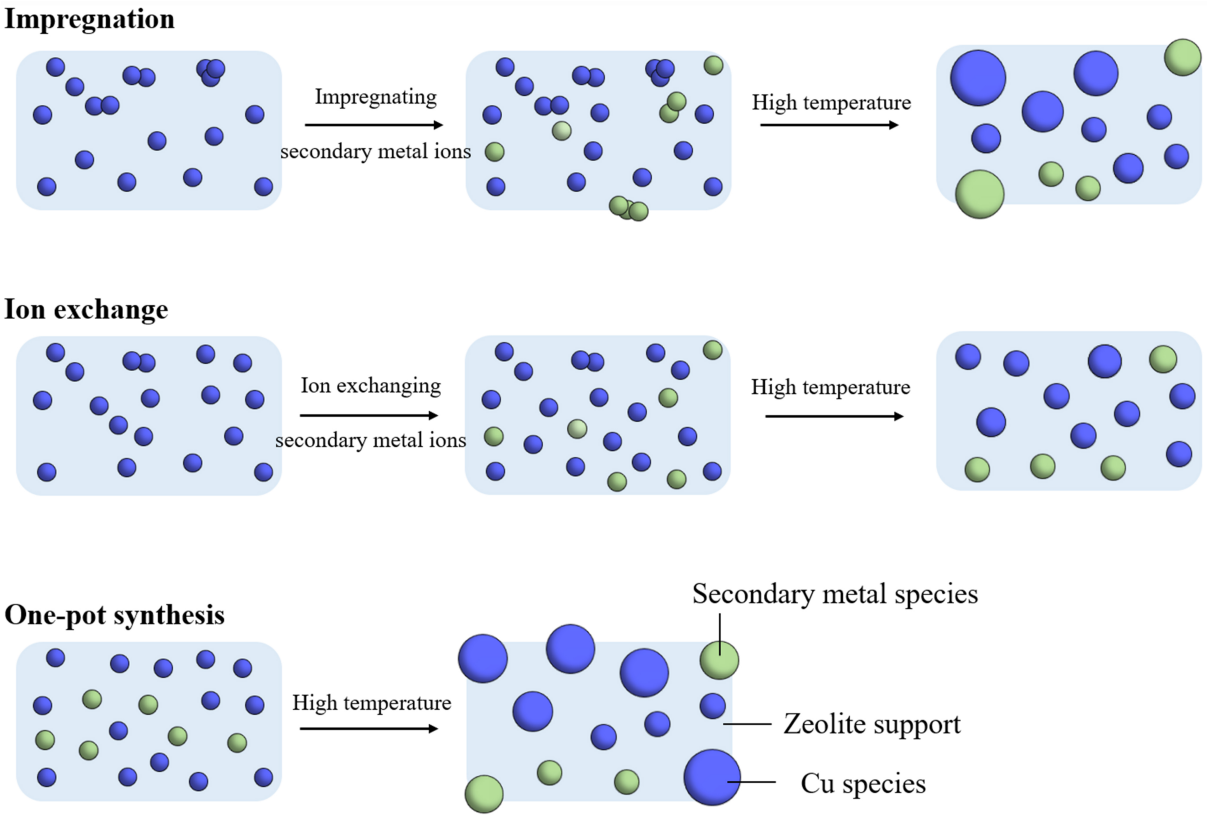

Figure 1. Different methods for introducing metal ions into zeolite crystallites.

tetraethylenepentamine (Cu-TEPA), as a replacement for the high-cost N,N,N-trimethyl-1-adamantammonium hydroxide (TMAdaOH)[82]. However, high Cu content in the initial synthesis system leads to the generation of undesired CuO_x after calcination, which prompts the development of routes to reduce the Cu loadings by post-treatment procedures such as HNO_3 treatment[83], NH_4NO_3 treatment[84] and HNO_3-NH_4NO_3 mixed treatment[85]. Therefore, it is essential to carefully choose a suitable strategy for the preparation of metal ions-exchanged zeolites.

Zhang *et al.* conducted a study on the preparation of Fe-Cu-SSZ-13 zeolites using a combination of one-pot synthesis, NH_4NO_3 treatment, and ion exchange methods[86]. Initially, Cu-SSZ-13 was synthesized using Cu-TEPA as the template. Subsequently, Cu-SSZ-13 was treated with NH_4NO_3 solution, followed by ion exchange with Fe ions. The obtained Fe-Cu-SSZ-13 displayed a wider operational temperature range and superior hydrothermal stability compared to Cu-SSZ-13. Characterization results indicated that Fe-Cu-SSZ-13 had fewer intracrystalline mass-transfer limitations, which are known to influence the low-temperature NH_3-SCR kinetics. The introduced Fe species primarily occurred in the outer regions of the SSZ-13 crystal, which was helpful for the reduction of intracrystalline mass-transfer limitations.

In another research conducted by Xu *et al.*, a Cu&Zn-SSZ-13(OP) catalyst with outstanding NH_3-SCR performance was synthesized using Cu&Zn-TEPA as the template through a one-pot method[87]. As depicted in Figure 2A, Cu&Zn-SSZ-13(OP) showed NO_x conversion exceeding 90% over a temperature range of 200-600 °C, which was broader than that of Cu-SSZ-13(OP) (200-550 °C). After undergoing hydrothermal aging, the catalytic activity of Cu&Zn-SSZ-13(OP) only displayed a slight decrease, whereas the activities of Cu-SSZ-13(OP) and ion-exchanged Cu&Zn-SSZ-13(IE) showed a significant reduction

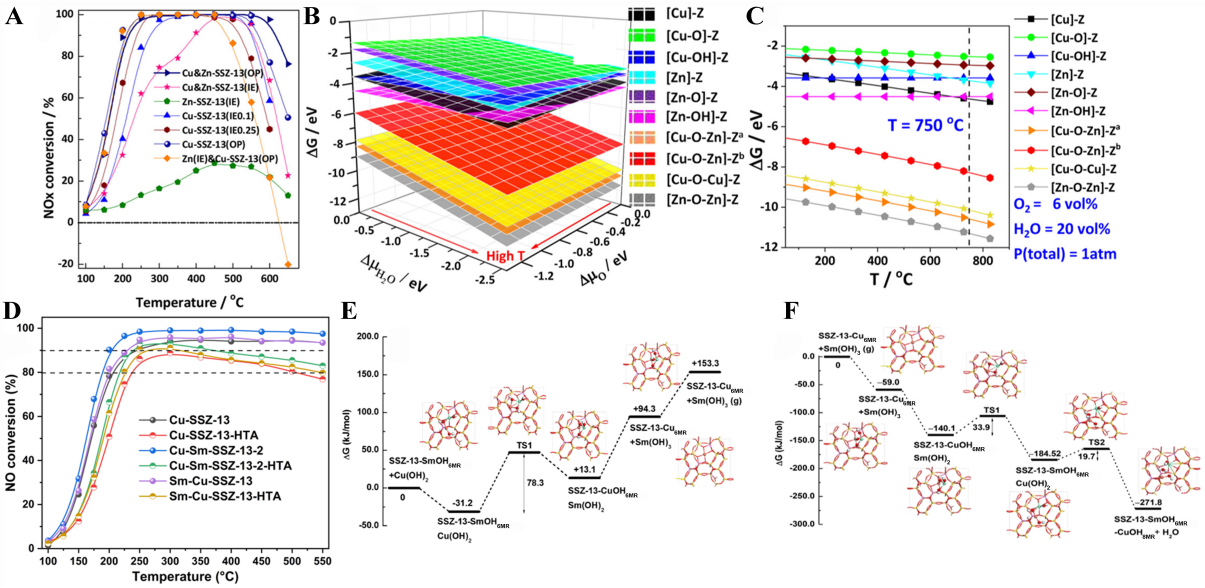

Figure 2. (A) NH_3-SCR curves of Cu-SSZ-13 and Cu&Zn-SSZ-13 zeolites; (B) DFT calculated reaction Gibbs free energies (ΔG) for different active centers; (C) ΔG values of active centers at different temperatures. Reproduced with permission from[87]. Copyright 2020, American Chemical Society; (D) NH_3-SCR curves of Cu-SSZ-13 and Cu-Sm-SSZ-13 zeolites; (E) ΔG profiles for replacement of $[Z_2Sm^{3+}(OH)]^{2+}$ ion at 6MR by Cu^{2+} ion; (F) ΔG profiles for replacement of Z_2Cu^{2+} ion at 6MR by Sm^{3+} ion. Reproduced with permission from[65]. Copyright 2022, American Chemical Society. NH_3-SCR: Ammonia-assisted selective catalytic reduction; DFT: density functional theory; 6MR: six-membered ring.

throughout the whole temperature and at high temperatures, respectively. Characterization studies indicated that the incorporation of Zn through a one-pot method favored the formation of isolated Cu^{2+} ions and various Zn-containing complexes. This was attributed to the reduced competition between Cu^{2+} and Zn^{2+} ions at ion-exchanged sites. Conversely, higher levels of CuO and ZnO species were found in Cu&Zn-SSZ-13(IE) because of the intense competition between the metal ions. Figure 2B presented the reaction Gibbs free energies (ΔG values) for the different active centers by density functional theory (DFT) calculations. Lower ΔG values indicated the greater stability of metallic complexes. Compared with Cu-SSZ-13(OP) and Cu&Zn-SSZ-13(IE), Cu&Zn-SSZ-13(OP) exhibited more stable complexes, which endowed it with higher hydrothermal stability. Figure 2C, which depicted the ΔG values as a function of temperature at fixed operating conditions, further supported the notion that Zn-containing complexes displayed higher hydrothermal stability than Cu complexes. This stability helped stabilize the framework and inhibit the migration of Cu^{2+} ions during hydrothermal aging, contributing to the superior hydrothermal stability of Cu&Zn-SSZ-13(OP).

Regarding the ion-exchange sequence, Jouini *et al.* demonstrated that preferential incorporation of Fe ions led to the generation of Fe_2O_3 and CuO nanoparticles within the zeolite[80]. However, when Cu ions were preferentially introduced, Fe-Cu nanocomposites and Fe_2O_3 particles were formed in the zeolite. This suggested that the order of metal exchange can affect the forms of metals in zeolites. Chen *et al.* discovered that Cu-Sm-SSZ-13, where Sm ions were introduced first followed by Cu ions, exhibited superior catalytic performance compared to Sm-Cu-SSZ-13[65]. As depicted in Figure 2D, Cu-Sm-SSZ-13 consistently outperformed Sm-Cu-SSZ-13 across the entire temperature range. It is particularly noteworthy that after undergoing hydrothermal aging, Cu-Sm-SSZ-13-2-HTA exhibited approximately 4% higher NO conversion compared to Sm-Cu-SSZ-13-HTA in the temperature range of 225-550 °C. DFT calculations were conducted to explore the effects of ion-exchange sequence to the locations of metal ions. As depicted in

Figure 2E, Sm ions were found to preferentially exchange with Z_2Cu^{2+} at the 6MR with a ΔG of -271.8 kJ/mol. Conversely, Cu ions encountered difficulty in exchanging $[Z_2Sm(OH)]^{2+}$ at the 6MR, as evidenced by a positive ΔG value of +153.3 kJ/mol [Figure 2F]. This suggested the higher stability of $[Z_2Sm(OH)]^{2+}$ ion at the 6MR. These findings emphasize the importance of the ion-exchange sequence in determining the distribution and forms of metals in zeolite catalysts.

In brief, the synthesis methods and ion-exchange sequence have great impacts on the forms and locations of metal ions in the zeolites. It is crucial to employ an appropriate strategy for introducing metal ions into zeolites to prevent the formation of undesired metal aggregates.

The importance of secondary metal ions content

The forms of secondary metal ions are affected by their content in zeolites[88-91]. Excessive amounts of these ions can lead to the formation of metal oxides, which can destroy the zeolite structure, trigger unwanted side reactions, and ultimately decrease the catalytic performance. In addition, more secondary metal ions generally require more ion-exchange sites in zeolites. This results in the competition with the Cu active sites, potentially leading to the generation of inactive CuO_x species. On the other hand, secondary metal ions fail to play effective roles when their loadings are low in zeolites. Therefore, it is necessary to determine the optimal content of these ions to maximize their functions.

Usui *et al.* conducted a study on the preparation of a collection of CuCe-SSZ-13 catalysts with varying Ce content ranging from 0.2 wt% to 5.0 wt% using an ion exchange method[64]. Figure 3A demonstrated that the relative crystallinity of the aged Cu-SSZ-13 sample was influenced by the Cu loadings. Following hydrothermal treatment at 700 °C, the zeolite structure remained largely unaffected regardless of the Cu loading. However, at a critical copper loading of 4.8 wt%, the zeolite structure started to degrade when the hydrothermal treatment was carried out at 750 °C. Further elevating the temperature to 850 °C led to a lower turning point of a copper loading of 2.6 wt%. Figure 3B demonstrated that Ce loadings below 1 wt% contributed to zeolite stability and maintained crystallinity even after severe hydrothermal tests. However, Ce loadings above 1 wt% led to zeolite structural damage and loss of crystallinity. Figure 3C clearly indicated that Ce content below 0.5 wt% was beneficial for stabilizing Cu-SSZ-13 after hydrothermal treatment at 850 °C. The optimal Ce loading was found to be approximately 0.35 wt %, resulting in 84% retention of crystallinity. NH_3-SCR performance of aged samples shown in Figure 3D indicated that CuCe-SSZ-13 with the optimal Ce loading displayed approximately 10% higher NO conversion than Cu-SSZ-13 and the zeolite with an excessively high Ce loading (5 wt%) over a wide range of temperatures. Transmission electron microscopy with energy-dispersive X-ray spectroscopy (TEM-EDX) was utilized to investigate the forms of Ce ions with different loadings. Figure 3E illustrated that at low Ce loading, the Ce species were observed to be uniformly dispersed across the SSZ-13 crystal and the detected concentration agreed with the actual Ce loading. However, as the Ce loading increased to approximately 5.0 wt%, the Ce species became less distributed and tended to aggregate into Ce oxides on the external surface of the crystal, leading to a decline in catalytic performance. Besides, the introduction of a higher content of La or Nb ions into Cu-SSZ-13 also resulted in the generation of metal oxides, which could block the channel, cover the Cu sites, and disrupt the zeolite structure, thereby decreasing catalytic properties[66,92].

Therefore, controlling the content of secondary metal ions in a reasonable manner can improve the catalytic properties of zeolites.

The interactions between secondary metal ions and Cu ions

The distribution of Cu ions

It is acknowledged that Z_2Cu^{2+} and $[ZCu(OH)]^+$ serve as the active sites for NH_3-SCR reaction[53-56].

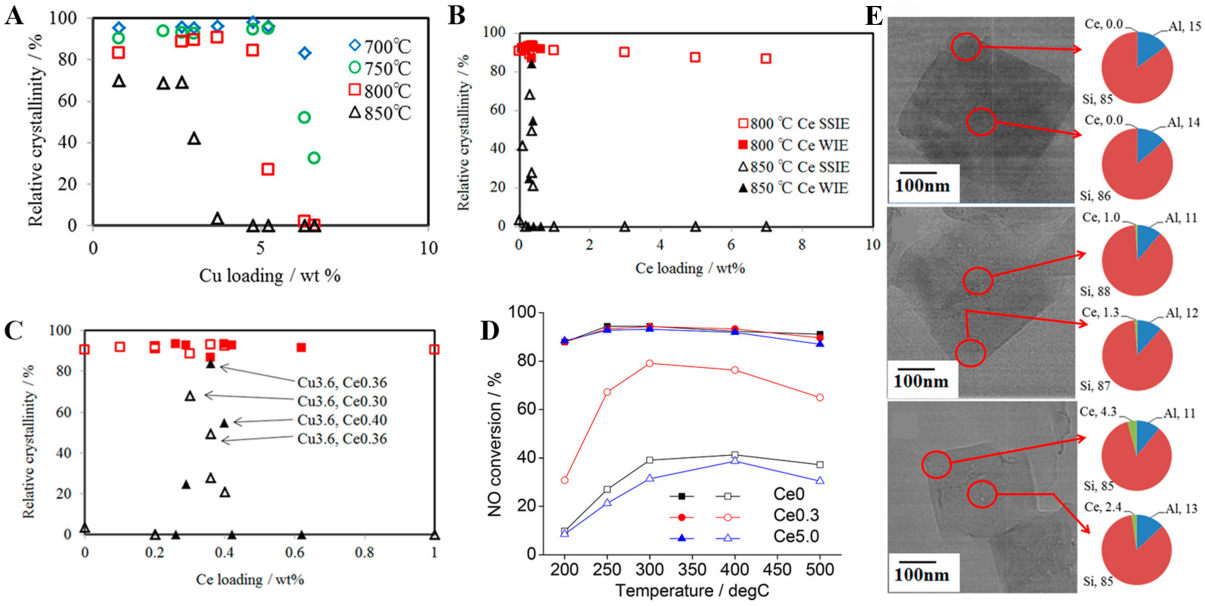

Figure 3. Impacts of (A) Cu loadings, (B) wide range of Ce loadings, and (C) short range of Ce loadings on the hydrothermal stability of zeolites; (D) Influence of Ce loadings on the SCR performance; (E) TEM-EDX results of CuCe-SSZ-13 zeolites with different Ce loadings. Reproduced with permission from[64]. Copyright 2018, American Chemical Society. SCR: Selective catalytic reduction; TEM-EDX: transmission electron microscopy with energy-dispersive X-ray spectroscopy.

$[ZCu(OH)]^+$ displays superior SCR activity attributed to its high mobility. In contrast, Z_2Cu^{2+} shows higher hydrothermal stability attributed to its strong coordination with the framework. In addition, $[ZCu(OH)]^+$ prefers to aggregate into CuO_x during severe hydrothermal treatment, leading to the destruction of the zeolite structure and a decrease in catalytic activity[59]. Consequently, regulating the distribution of Cu ions directly influences the catalytic performance of the catalysts.

Alkali metal ions play a crucial role in zeolite synthesis, with some alkali metals acting as templates to direct the synthesis of target zeolites. However, during catalytic test, residual alkali metals often poison and deactivate the catalysts. Fortunately, Zhu *et al.* demonstrated the positive role of Na^+ in enhancing the catalytic performance of Cu-SSZ-13 catalyst[93]. Figure 4A depicted the temperature-programmed reduction of hydrogen (H_2-TPR) profiles of samples. A distinct peak below 500 °C, assigned to the reduction of $[ZCu(OH)]^+$, could be observed in Cu-SSZ-13 with the presence of Na^+, suggesting that Na^+ promoted the formation of $[ZCu(OH)]^+$. Ultraviolet-visible (UV-vis) spectrum analysis indicated that CuNa-SSZ-13 exhibited a higher quantity of Cu^{2+} compared to Cu-SSZ-13 [Figure 4B]. DFT calculations confirmed that Na ions improved the stability of Cu-SSZ-13, as evidenced by a lower energy of -878.3157 eV compared to Cu-SSZ-13(-878.2358 eV) [Figure 4C]. Additionally, Na ions facilitated the migration of Cu species from 6MRs to 8MRs, providing a lower exchange energy of 9.61 kJ/mol compared to Cu-SSZ-13 (29.45 kJ/mol). As a result, CuNa-SSZ-13 displayed 7% and 30% higher NO_x conversion at 150 and 180 °C, respectively, compared to Cu-SSZ-13 [Figure 4D]. After hydrothermal aging, the activity of CuNa-SSZ-13-HA exhibited a slight decrease compared to its counterpart. While the activity of Cu-SSZ-13-HA showed an obvious decrease across the entire temperature range. Kinetic experiments shown in Figure 4E further confirmed that CuNa-SSZ-13, with a higher activation energy of 51.7 kJ/mol, exhibited more active sites and a more completed reaction mechanism compared to Cu-SSZ-13 (42.2 kJ/mol).

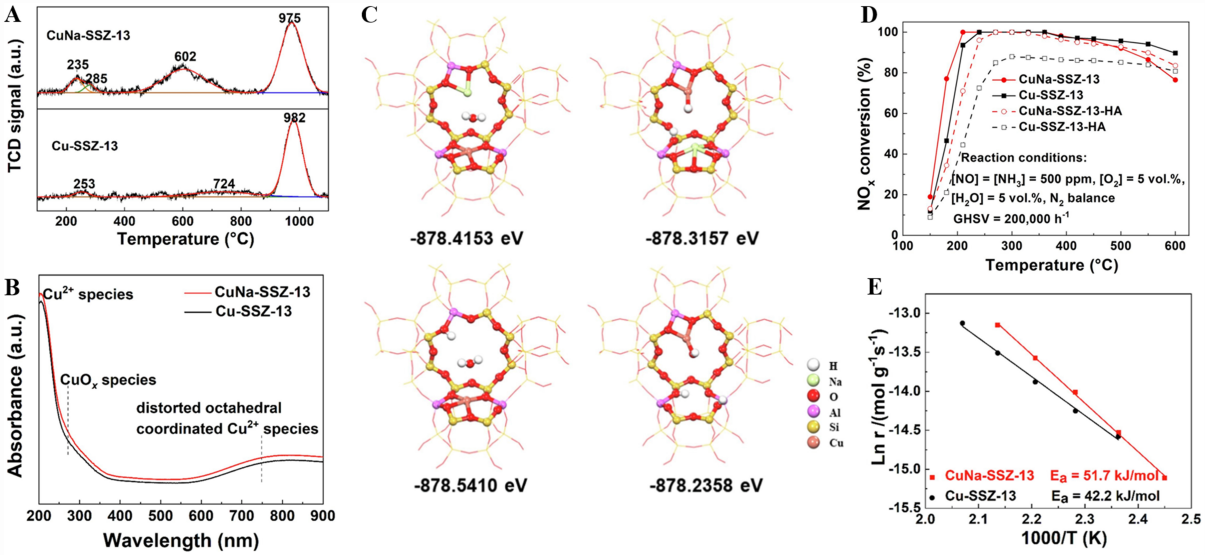

Figure 4. H_2-TPR profiles (A) and UV-vis DRS spectra (B) of zeolite catalysts; (C) Simulated positions of Cu ions and alkali metals in the zeolite; NH_3-SCR curves (D) and Arrhenius plots (E) of zeolite catalysts. This figure is quoted with permission from Elsevier[93]. H_2-TPR: Temperature-programmed reduction of hydrogen; UV-vis: ultraviolet-visible; DRS: diffuse reflectance spectroscopy; NH_3-SCR: ammonia-assisted selective catalytic reduction.

Furthermore, Lv *et al.* conducted a study where they synthesized SSZ-13 zeolites using various alkali metal cations[94]. The findings revealed that there was an increase in the amount of paired Al species and distorted Al tetrahedra with the reduced radii of alkali metal cations. This, in turn, resulted in an increase in isolated Cu^{2+} species near 6MRs and improved catalytic performance in NH_3-SCR. The increased isolated Cu^{2+} species near 6MRs benefited the enhanced NH_3-SCR performance.

Recently, Chen *et al.* reported that doping Sm ions into SSZ-13 could enhance its low-temperature activity[65]. X-ray diffraction (XRD) Rietveld refinement and aberration-corrected TEM revealed that the added Sm ions occupied at the 6MRs. H_2-TPR was employed to investigate the distribution of Cu active sites. As depicted in Figure 5A, $[ZCu(OH)]^+$, CuO_x, Z_2Cu^{2+} and Cu^+ appeared in Cu-SSZ-13 and Cu-Sm-SSZ-13 zeolites. Z_2Cu^{2+} displayed a higher reduction temperature compared to $[ZCu(OH)]^+$. Figure 5B showed that the amount of $[ZCu(OH)]^+$ increased accompanying the decrease of Z_2Cu^{2+} and constant CuO_x content as the Sm ions loadings rose. These results suggested that the initially introduced Sm ions facilitated the migration of subsequently introduced Cu ions to the 8MRs to form $[ZCu(OH)]^+$. Consequently, Cu-Sm-SSZ-13 with more amount of $[ZCu(OH)]^+$ exhibited a wider temperature window (200-550 °C) for achieving NO conversion above 90% (T_{90}) compared to that of Cu-SSZ-13 (250-550 °C) [Figure 5C]. Moreover, the group also demonstrated that Cu-La-SSZ-13 exhibited superior hydrothermal stability compared to Cu-SSZ-13 under the same treatment conditions[66]. DFT calculations revealed that La ions were situated at the 8MRs of SSZ-13, forming $[ZLa(OH)_2]^+$ species. This resulted in an increased presence of Z_2Cu^{2+} at 6MRs [Figure 5D]. This observation was consistent with the H_2-TPR results, which showed an elevation in the percentage of Z_2Cu^{2+} from 51% to 62% upon the introduction of La^{3+} [Figure 5E]. Consequently, after high-temperature hydrothermal aging, NO conversion of Cu-La-SSZ-13-HTA containing more amount of Z_2Cu^{2+} was around 5%-10% higher than that of Cu-SSZ-13-HTA at high temperatures (400-550 °C) [Figure 5F].

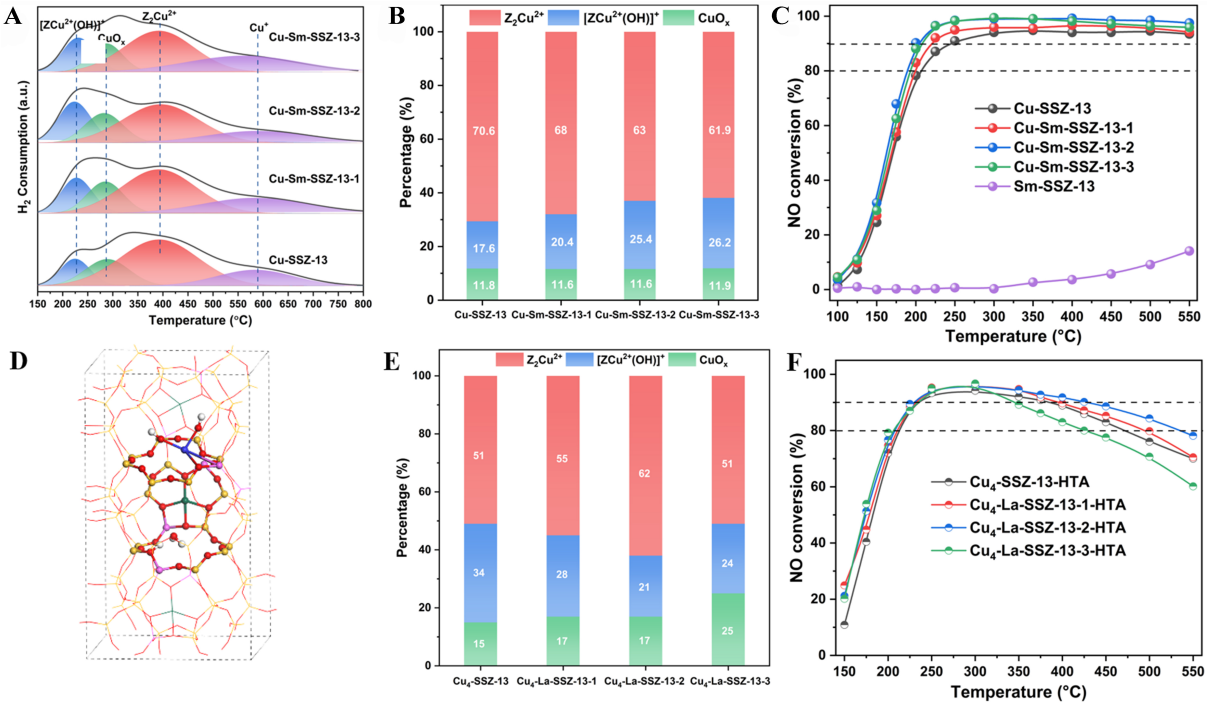

Figure 5. H_2-TPR profiles (A) and Cu distribution (B) of different zeolites; (C) NH_3-SCR curves at various temperatures for distinct zeolites before high-temperature hydrothermal aging. Reproduced with permission from[65]. Copyright 2022, American Chemical Society; (D) DFT-optimized structures of Cu-La-SSZ-13 zeolite; (E) Cu distribution of different zeolites; (F) NH_3-SCR curves at varying temperatures for different zeolites after hydrothermal aging. This figure is quoted with permission from Springer[66]. H_2-TPR: Temperature-programmed reduction of hydrogen; NH_3-SCR: ammonia-assisted selective catalytic reduction; DFT: density functional theory.

Indeed, transition metal ions also play a significant function in adjusting the distribution of Cu ions within SSZ-13 zeolite. Lee *et al.* observed that Cu(*x*)Co-SSZ-13 displayed better activity at low temperatures compared to Cu(*x*)-SSZ-13, despite Co-SSZ-13 showing poor SCR activity[95]. Diffuse reflectance infrared Fourier transform (DRIFT) spectroscopy demonstrated that pre-loaded Co ions preferred to occupy the 6MRs of SSZ-13 [Figure 6A]. H_2-TPR analysis [Figure 6B] presented two obvious peaks. The first peak at low temperatures (200-300 °C) was due to the reduction of $[ZCu(OH)]^+$ while the second peak at high temperatures (350-500 °C) was attributed to the reduction of Z_2Cu^{2+}. Compared to Cu(*x*)-SSZ-13, Cu(*x*)Co-SSZ-13 displayed an increased peak below 300 °C and a decreased peak above 350 °C, suggesting a higher amount of $[ZCu(OH)]^+$. Additionally, Figure 6C indicated that all Cu species were present as Cu^{2+} in the zeolites, without the presence of CuO_x. These characteristics resulted in Cu(0.5)Co-SSZ-13 exhibiting a reaction rate 92% higher than that of Cu(0.5)-SSZ-13 at 250 °C [Figure 6D]. Besides, because of a smaller ionic radius of Nb ions relative to Cu ions, Nb ions preferred to occupy the 6MRs of SSZ-13[92]. This led to an increased amount of $[ZCu(OH)]^+$ in $Nb_{0.7\%}/Cu_{2\%}$-SSZ-13 [Figure 6E]. This catalyst exhibited an average of 22.7% higher NO conversion than $Cu_{2\%}$-SSZ-13 at temperatures ranging from 200 to 275 °C [Figure 6F]. Interestingly, it achieved a NO conversion of 67% at 150 °C, which was close to the targets of "The 150 °C Challenge"[96].

Therefore, the catalytic properties of zeolites can be enhanced by regulating the distribution of Cu active sites by introducing the secondary metal ions.

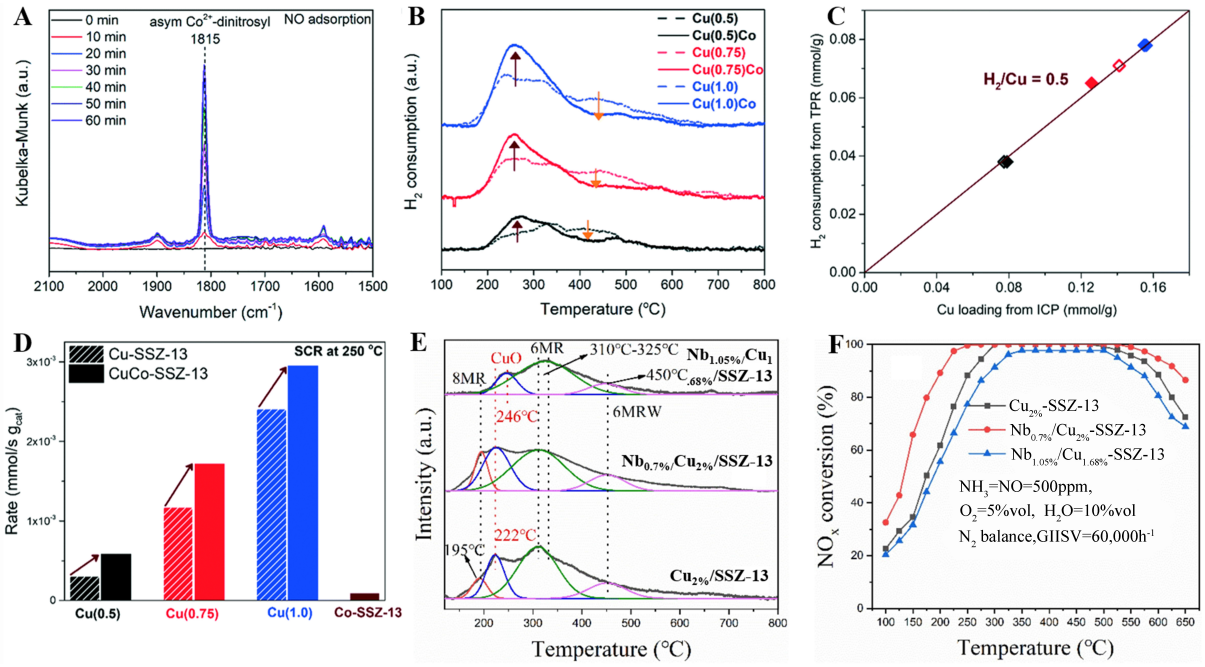

Figure 6. (A) NO-DRIFT spectra of Co-SSZ-13 zeolite; (B) H_2-TPR profiles of Cu-SSZ-13 and CuCo-SSZ-13; (C) Correlation between H_2 consumption and Cu content; (D) NO_x removal rate at 250 °C of Cu-SSZ-13 and CuCo-SSZ-13 zeolites. This figure is quoted with permission from the Royal Society of Chemistry[95]; H_2-TPR profiles (E) and catalytic performances (F) of three different catalysts. This figure is quoted with permission from Elsevier[92]. DRIFT: Diffuse reflectance infrared Fourier transform; H_2-TPR: temperature-programmed reduction of hydrogen.

The stability of Cu ions

During high-temperature hydrothermal aging, Cu ions have a tendency to migrate and aggregate into inactive CuO_x, which can lead to the damage of the zeolite structure and result in the occurrence of side reactions, leading to inferior NH_3-SCR catalytic performance[59,97-100]. Mechanistically, Z_2Cu^{2+} or $[ZCu(OH)]^+$ can undergo one or two-step reactions with H_2O to generate $Cu(OH)_2$. Subsequently, $Cu(OH)_2$ species move outside the zeolite, gradually transforming into CuO_x and destroying the zeolite skeleton. Especially, $[ZCu(OH)]^+$ is more prone to transforming into CuO_x during hydrothermal aging due to its high mobility and one-step reaction process. Inhibiting the migration of Cu ions and stabilizing their presence are crucial for maintaining the hydrothermal stability of zeolites.

Cui *et al.* prepared a series of Cu,M/SSZ-13 (M = Na^+, K^+ and Ca^{2+}) zeolites by solution ion exchange[101]. The relative crystallinities shown in Figure 7A indicated that incorporating Na^+ or K^+ did not significantly influence the zeolite crystallinity except when the M/Cu ratio reached 1.0. However, the introduction of Ca^{2+} significantly led to a significant reduction in zeolite crystallinity. The catalytic results on hydrothermal-aged zeolites [Figure 7B] demonstrated that Cu,K/SSZ-13 and Cu,Na/SSZ-13 exhibited NO_x conversion above 90% within the temperature window of 200-500 °C. On the contrary, Cu,H/SSZ-13 and Cu,Ca/SSZ-13 displayed inferior catalytic activity at high temperatures (> 400 °C). The measured apparent activation energies of Cu,Na/SSZ-13 and Cu,K/SSZ-13 decreased from 70 to 55 kJ/mol with the increasing co-cation concentrations [Figure 7C]. However, the introduction of Ca^{2+} did not influence the apparent activation energies. Turnover rates (TORs) presented in Figure 7D indicated that the TORs of Cu,Na-SSZ-13 and Cu,K/SSZ-13 were extraordinarily higher than that of Cu,H/SSZ-13 at M/Cu ratios = 0.7 and 1.0. However, the TORs decreased with increasing Ca^{2+} content in Cu,Ca/SSZ-13. The distribution of Cu species depicted in Figure 7E showed that the content of electron paramagnetic resonance (EPR)-active Cu sites initially

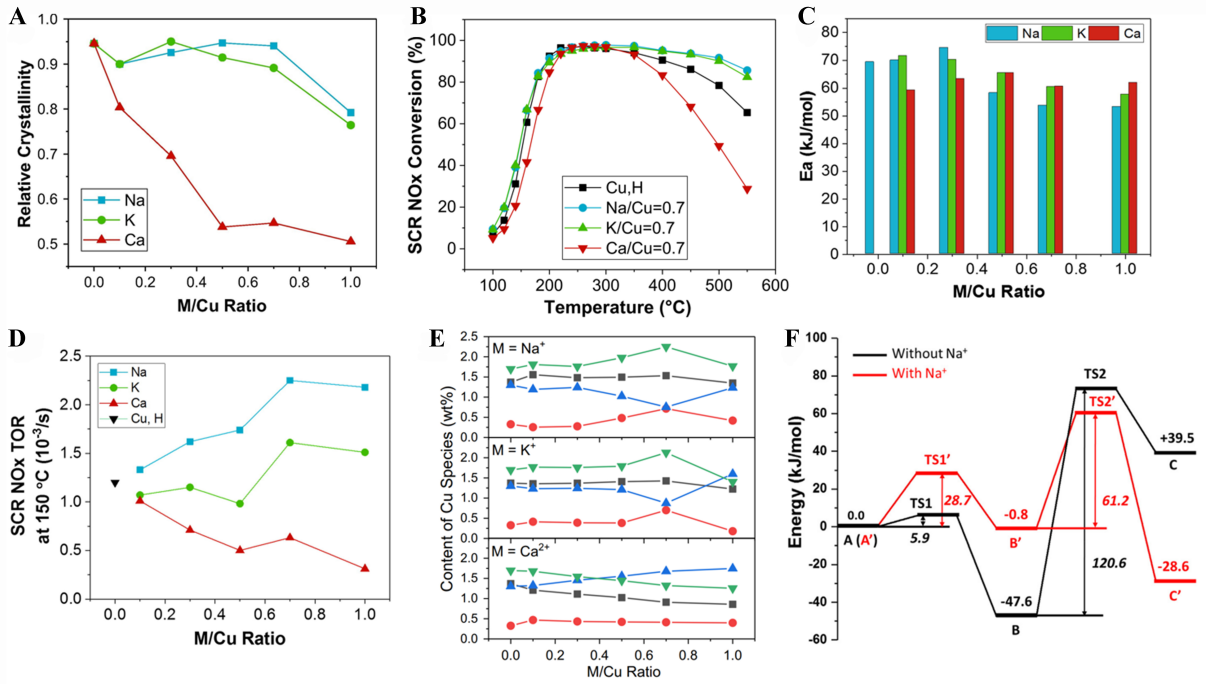

Figure 7. Relative crystallinity (A) and NH_3-SCR curves (B) of hydrothermally-aged zeolite catalysts; (C) Apparent activation energies at low temperatures for aged zeolite catalysts; (D) TORs of different zeolite catalysts at 150 °C; (E) Different Cu species content of aged zeolite catalysts. Z_2Cu^{2+} (■), $[ZCu(OH)]^+$ (●), total Cu sites (▼), CuO_x (▲); (F) ΔG for $[ZCu(OH)]^+$ hydrolysis to $Cu(OH)_2$ with and without Na^+. This figure is quoted with permission from Elsevier[101]. NH_3-SCR: Ammonia-assisted selective catalytic reduction; TORs: turnover rates.

increased and then decreased with the increase of alkali metal ion content. In contrast, the content of both Z_2Cu^{2+} and total EPR active Cu sites declined with increasing Ca loading. In addition, the effects of overloaded Na^+ and K^+ in the catalysts were investigated. As shown in Figure 7F, the presence of excess alkali metal ions destabilized the $[ZCu(OH)]^+$ and facilitated the formation of CuO_x clusters. Conversely, the co-cation Ca^{2+} destabilized the highly stable Z_2Cu^{2+} via site competition. These comprehensive investigations unveiled that the addition of alkali metal ions can be utilized in the synthesis of Cu/SSZ-13 catalysts that are highly stable and active. Furthermore, DFT calculations revealed the repulsive interactions between Cu sites and alkali metal ions that can prevent the high loadings of Cu ions.

Very recently, Kang *et al.* conducted a study involving the preparation of a series of Cu/Yx-SSZ-13 zeolites. They discovered that Cu/Y_4-SSZ-13 with 0.42 wt% Y loading exhibited higher hydrothermal stability compared to Cu-SSZ-13[67]. Y ions were first doped using an in-situ method and then Cu ions were introduced by an ion-exchange process in their experimental procedure. A high-angle annular dark-field scanning transmission electron microscopy (HAADF-STEM) image revealed clear and distinct bright dots, representing individual Y atoms, with higher contrast compared to surrounding zeolite framework. This obversion strongly suggested the presence of Y cations at 6MRs of SSZ-13 [Figure 8A]. H_2-TPR profiles showed that the populations of $[ZCu(OH)]^+$ in 8MRs increased with the Y loadings, reaching a maximum of 56% for Cu/Y_4-SSZ-13 [Figure 8B]. NH_3-DRIFT spectra further supported the presence of more $[ZCu(OH)]^+$ in the 8MRs of Cu/Y_4-SSZ-13 [Figure 8C]. This increase was primarily attributed to the steric hindrance caused by Y ions at 6MRs. Mechanism studies revealed that the ΔG values for the generation of $Cu(OH)_2$ during hydrothermal aging were 0.83 eV for Cu-SSZ-13 and 1.60 eV for Cu/Y_4-SSZ-13, indicating that Y ions raised the reaction barrier for Cu ions to transform into $Cu(OH)_2$ [Figure 8D]. In other words, Y

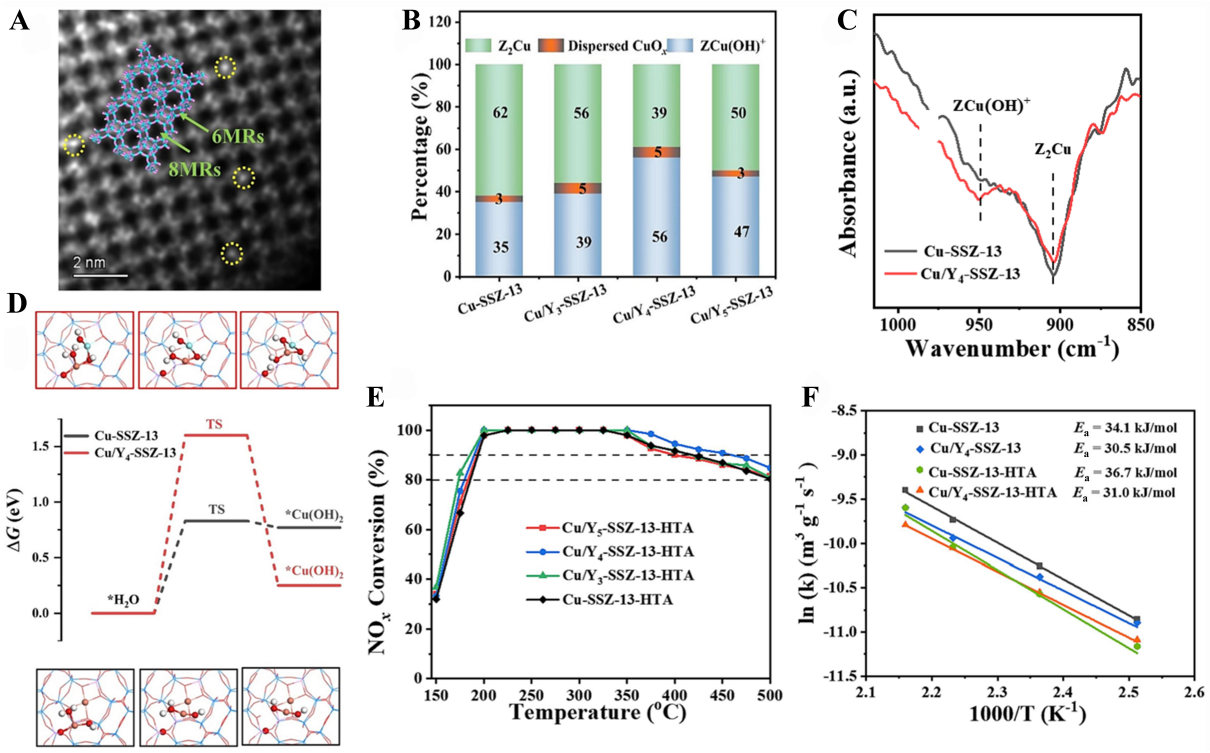

Figure 8. (A) HAADF-STEM image of Y_4-SSZ-13 along the [211] zone axis; (B) Cu distribution, (C) NH_3-DRIFT spectra of T-O-T region, and (D) Δ*G* values for the generation of $Cu(OH)_2$ of zeolite catalysts; NH_3-SCR curves (E) and Arrhenius plots (F) of Cu-SSZ-13 and Cu/Y_4-SSZ-13. This figure is quoted with permission from Elsevier[67]. HAADF-STEM: High-angle annular dark-field scanning transmission electron microscopy; DRIFT: diffuse reflectance infrared Fourier transform; NH_3-SCR: ammonia-assisted selective catalytic reduction.

ions could inhibit the aggregation of Cu ions. NH_3-SCR results demonstrated that Cu/Y_4-SSZ-13-HTA achieved a remarkable 76% NO conversion at 175 °C and an impressive 91% NO conversion at 450 °C, surpassing the performance of Cu-SSZ-13-HTA, which exhibited 66% and 86% NO conversion at the same temperatures, respectively [Figure 8E]. Arrhenius plots and corresponding apparent activation energies were presented in Figure 8F. It is noteworthy that Cu/Y_4-SSZ-13 catalysts exhibited lower *Ea* values compared to Cu-SSZ-13. This finding indicated that the presence of Y ions enhanced the redox capabilities of Cu species, resulting in improved reactivities.

Additionally, Chen *et al.* conducted studies on Cu-Sm-SSZ-13-HTA and reported that it exhibited a maintained T_{90} window at the temperature range of 250-350 °C, while the NO conversion of Cu-SSZ-13-HTA dropped below 90% across the entire temperature range after severe hydrothermal treatment[65]. Spectral characterization studies indicated that Cu-Sm-SSZ-13-HTA preserved more Cu^{2+} sites and fewer CuO_x species compared to Cu-SSZ-13-HTA. Furthermore, DFT calculations revealed that the Δ*G* value for the transformation of $[ZCu(OH)]^+$ into CuO_x could be increased by 41.6 kJ/mol in Cu-Sm-SSZ-13 compared to Cu-SSZ-13. This enhanced stability of $[ZCu(OH)]^+$ was beneficial for improving hydrothermal stability of Cu-Sm-SSZ-13.

Apart from inhibiting the migration of $[ZCu(OH)]^+$, enhancing the stability of Z_2Cu^{2+} also contributes to the hydrothermal stability of zeolites. Chen *et al.* demonstrated that Cu-La-SSZ-13 displayed superior hydrothermal stability in comparison to Cu-SSZ-13[66]. DFT calculation results indicated that the intrinsic stability of Z_2Cu^{2+} could be promoted after doping La ions. The reaction energy barrier for transforming

Z_2Cu^{2+} into CuO_x could be increased by 108 kJ/mol in Cu-La-SSZ-13 compared to Cu-SSZ-13. This increase effectively inhibited the formation of CuO_x. Furthermore, the results of dealumination process studies indicated that ΔG values for four Al–O bond-breaking steps in La-SSZ-13 were 28.4, 7.1, 11.1, and 43.4 kJ/mol higher than those in H-SSZ-13, respectively. These findings provided evidence that Cu-La-SSZ-13 displayed superior hydrothermal stability. Similarly, the addition of Pr ions was found to promote the hydrothermal stability of Cu-SSZ-13[102]. XRD Rietveld refinement showed that Pr ions occupied the 8MRs. DFT calculations revealed that the initial reaction energy barriers for transforming Z_2Cu^{2+} into CuO_x in Cu-SSZ-13 were certain values [Figure 9A]. However, after doping Pr ions, the reaction energy barriers increased, confirming that Pr ions effectively inhibited the migration and aggregation of Z_2Cu^{2+} during hydrothermal aging. To investigate the broader applicability of secondary cations located at 8MRs in enhancing hydrothermal stability, the researchers further conducted DFT calculations by introducing Ce into Cu-SSZ-13 zeolites. The calculations demonstrated that the addition of Ce raised the hydrolysis barrier for the Z_2Cu^{2+} ions located in the 6MRs, resulting in improved hydrothermal stability [Figure 9B].

Therefore, improving the stability of Cu ions, suppressing the migration of Cu ions, and decreasing the generation of CuO_x can promote the hydrothermal stability of zeolites.

The activity of Cu ions

It is widely recognized that Cu ions undergo a redox cycle during NH_3-SCR reaction. Mechanistically, improving the reactivity of Cu ions and accelerating the formation and decomposition of intermediate products significantly influence the catalytic activity of catalysts. Additionally, due to the presence of ammonia solvation and ammonia inhibition, Cu ions usually fail to reduce NO_x at low temperatures (< 200 °C)[103-108]. Therefore, boosting the reactivity of Cu ions represents an effective approach for enhancing low-temperature activity of zeolites.

Recently, the influence of Sm ions on the activity of $[ZCu(OH)]^+$ was demonstrated[65]. X-ray photoelectron spectroscopy (XPS) made clear that Cu-Sm-SSZ-13 exhibited a higher electronegativity of Cu^{2+} ions compared to Cu-SSZ-13. DFT calculations provided further insights, showing a decrease in Bader charges of $[ZCu(OH)]^+$ from +1.070 to +0.943 |e| in the presence of Sm ions at 6MRs, accompanied by an increased Bader charge of Sm ions from +2.082 to +2.276 |e|. These computational results were consistent with the experimental observations, indicating charge transfer from Cu to Sm ions. Moreover, increased electronegativity of $[ZCu(OH)]^+$ resulted in reduced activation energies for the formation of H_2NNO and HONO intermediates. Specifically, the activation energies for the formation of H_2NNO and HONO decreased from 56.7 to 31.4 kJ/mol and from 69.7 to 39.5 kJ/mol with the addition of Sm ions, respectively. This reduction in activation energy suggested enhanced activity of $[ZCu(OH)]^+$. As a result, Cu-Sm-SSZ-13 displayed approximately 10% higher NO conversion than Cu-SSZ-13 from 175 to 250 °C.

Kang *et al.* reported that Cu/Y_4-SSZ-13 achieved 84% NO conversion at 175 °C, surpassing the 70% conversion achieved by Cu-SSZ-13[67]. H_2-TPR results indicated a shift in the reduction temperature of Cu^{2+} active sites towards lower values by 20-30 °C upon the addition of Y ions, suggesting enhanced reducible ability. This observation was consistent with findings reported in other literature[63,66]. XPS results also indicated the increased Binding Energy value of Cu ions with the addition of Y ions, implying the decreased electron density of Cu ions. This phenomenon facilitated the SCR reaction rate by adsorbing more accessible NH_3. DFT calculations shown in Figure 10 further indicated that the ΔG values for the formation of HONO and H_2NNO intermediates decreased from 1.01 to 0.86 eV and from 1.71 to 0.77 eV, respectively, after doping Y ions into Cu-SSZ-13. These findings clearly highlighted the enhanced the activity of $[ZCu(OH)]^+$ in the presence of Y ions.

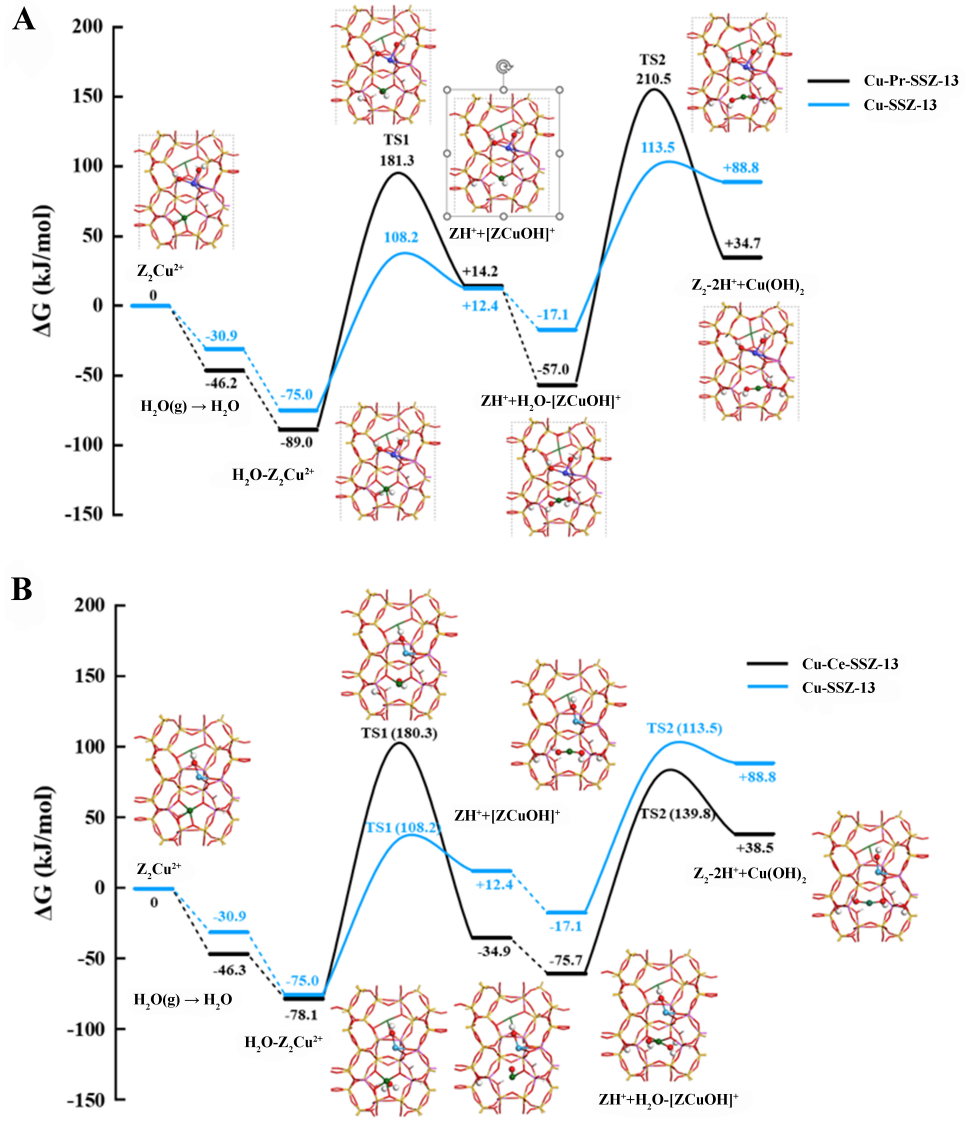

Figure 9. DFT calculated Δ*G* values for the transformation of Z_2Cu^{2+} ions with or without (A) $[ZPr^{3+}(OH)_2]^+$ and (B) $[ZCe^{3+}(OH)_2]^+$ during hydrothermal aging. This figure is quoted with permission from the Royal Society of Chemistry[102]. DFT: Density functional theory.

Although enhancing the reactivity of Cu ions can indeed promote the catalytic activity of zeolites, there is a lack of research specifically exploring the reactivity of Cu ions. However, placing emphasis on the activity of Cu ions can provide valuable insights into the reaction mechanism and the roles of secondary metal ions.

CONCLUSION AND OUTLOOK

It is widely accepted that Z_2Cu^{2+} and $[ZCu(OH)]^+$ play a key function in determining the catalytic performance of zeolite catalysts. Fortunately, introducing secondary metals into Cu-SSZ-13 zeolites offers a straightforward and effective approach to improve the NH_3-SCR performance of zeolites. This method allows for the control of the activity, stability and distribution of Cu active sites. Generally, increasing the quantity of $[ZCu(OH)]^+$ and improving the activity of Cu sites benefits the enhancement of catalytic activity in zeolites. On the other hand, increasing the amount of Z_2Cu^{2+} and enhancing the stability of Cu sites

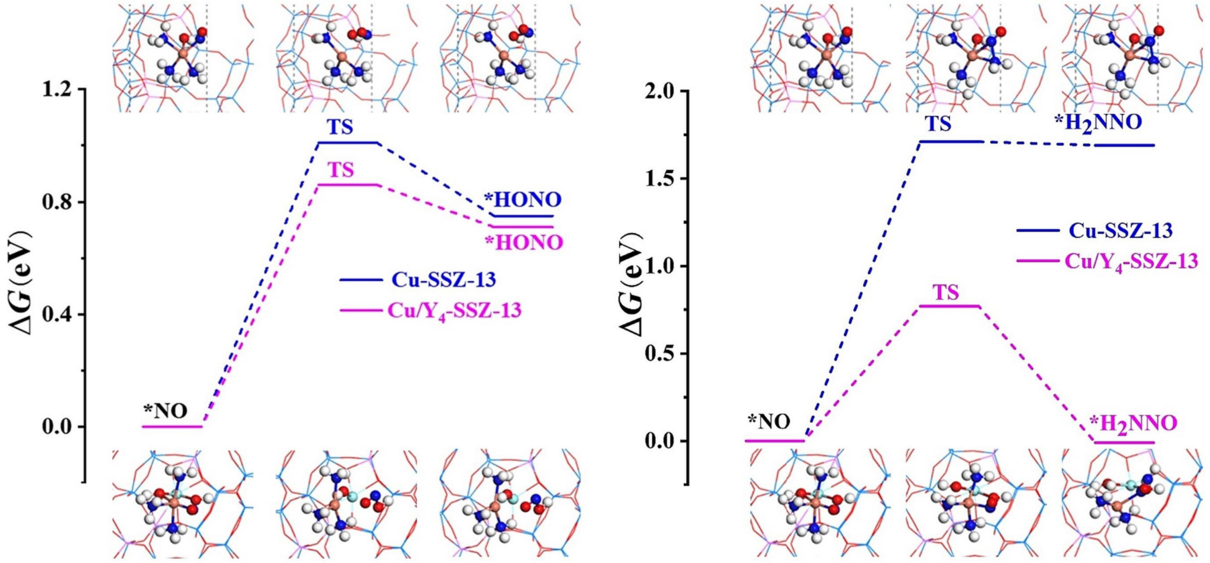

Figure 10. DFT calculated ΔG values for the formation of HONO and H_2NNO intermediates on the $ZCu^{2+}(OH)(NH_3)_3$ site of Cu-SSZ-13 zeolites with or without Y ions. This figure is quoted with permission from Elsevier[67]. DFT: Density functional theory.

contribute to the hydrothermal stability of zeolites. However, it is crucial to note that the efficacy of this approach relies on the strategy and content of introducing metal ions. Improper introduction or inappropriate content of metal ions can lead to the generation of inactive CuO_x species, resulting in a decline in both catalytic activity and hydrothermal stability of zeolites. Therefore, this review concentrates on recent developments in bimetallic zeolites for the NH_3-SCR reaction with the aim of providing insights into the strategies and advancements for enhancing the catalytic performance of zeolites.

To gain a clear understanding of the functions and operational mechanisms of secondary metal ions at the molecular level, advanced atomic-resolution characterization techniques accompanying DFT calculations need to be developed to monitor Cu active sites and simulate reaction mechanisms. These approaches can help design high-performance NH_3-SCR catalysts with excellent durability. Some perspectives are proposed to in this fascinating area, including: (1) Introducing multiple metal ions into Cu-SSZ-13 to achieve better regulation of Cu site properties and enhance catalytic performance. For instance, a Cu-Ce-La-SSZ-13 zeolite prepared using a one-pot method demonstrated superior catalytic performance compared to Cu-SSZ-13 and ion-exchanged synthesized Cu-Ce-La/SSZ-13[109]. This improvement was attributed to the effective restraint of Cu^{2+} ion migration by Ce^{4+} and La^{3+} introduced into the cages of SSZ-13 through the one-pot method; (2) Searching for cost-effective and facile routes to prepare bimetallic zeolites. Researchers have synthesized FeCu-SSZ-13 zeolites using inexpensive diatomite as a source of silicon and iron[110,111]. In addition, SSZ-13 zeolite can be rapidly synthesized using scrap material coal gangue as the source of silicon and Al[112]; (3) Investigating alternative cost-effective small-pore zeolites, considering the high cost associated with the synthesis of SSZ-13 zeolites; (4) Further investigating the mechanism by which secondary metal ions influence the activity of Cu active sites at low temperatures; (5) Continuously exploring additional impacts of secondary metal ions, such as modifying the acidity of the zeolite and impeding the dealumination of the zeolite framework during hydrothermal treatment.

In conclusion, bimetallic zeolite catalysts are anticipated to find broader applications in exhaust aftertreatment systems, leveraging their superior catalytic activity and hydrothermal stability. These catalysts hold great potential for addressing the challenges associated with emission control and pollutant

removal in various industries.

DECLARATIONS

Authors' contributions

Prepared and revised the manuscript: Chen, M.
Revised the manuscript: Ren, S. B.; Han, D. M.
Designed and revised the manuscript: Chen, M.

Availability of data and materials

Not applicable.

Financial support and sponsorship

This work was supported by the National Natural Science Foundation of China (22301209, 21976129) and the Zhejiang Provincial Natural Science Foundation of China (LQ20B010004, ZCLQ24B0101).

Conflicts of interest

All authors declared that there are no conflicts of interest.

Ethical approval and consent to participate

Not applicable.

Consent for publication

Not applicable.

REFERENCES

1. Richter, A.; Burrows, J. P.; Nüss, H.; Granier, C.; Niemeier, U. Increase in tropospheric nitrogen dioxide over China observed from space. *Nature* **2005**, *437*, 129-32. DOI PubMed
2. Kim, C. H.; Qi, G.; Dahlberg, K.; Li, W. Strontium-doped perovskites rival platinum catalysts for treating NO_x in simulated diesel exhaust. *Science* **2010**, *327*, 1624-7. DOI PubMed
3. Han, L.; Cai, S.; Gao, M.; et al. Selective catalytic reduction of NO_x with NH_3 by using novel catalysts: state of the art and future prospects. *Chem. Rev.* **2019**, *119*, 10916-76. DOI
4. Shan, Y.; Du, J.; Zhang, Y.; et al. Selective catalytic reduction of NO_x with NH_3: opportunities and challenges of Cu-based small-pore zeolites. *Natl. Sci. Rev.* **2021**, *8*, nwab010. DOI PubMed PMC
5. Wei, Y.; Wang, S.; Chen, M.; et al. Coaxial 3D printing of zeolite-based core-shell monolithic Cu-SSZ-13@SiO_2 catalysts for diesel exhaust treatment. *Adv. Mater.* **2024**, *36*, e2302912. DOI PubMed
6. Chen, M.; Bi, J.; Liu, C.; Ren, S. Enhancing performance of Fe-SSZ-13 and Cu-Fe-SSZ-13 zeolites for selective catalytic reduction reaction via post-treatment method. *Mater. Lett.* **2023**, *349*, 134872. DOI
7. Twigg, M. V. Progress and future challenges in controlling automotive exhaust gas emissions. *Appl. Catal. B. Environ.* **2007**, *70*, 2-15. DOI
8. Zhang, R.; Liu, N.; Lei, Z.; Chen, B. Selective transformation of various nitrogen-containing exhaust gases toward N_2 over zeolite catalysts. *Chem. Rev.* **2016**, *116*, 3658-721. DOI PubMed
9. Beale, A. M.; Gao, F.; Lezcano-Gonzalez, I.; Peden, C. H.; Szanyi, J. Recent advances in automotive catalysis for NO_x emission control by small-pore microporous materials. *Chem. Soc. Rev.* **2015**, *44*, 7371-405. DOI PubMed
10. Chen, M.; Sun, Q.; Yang, G.; et al. Enhanced performance for selective catalytic reduction of NO_x with NH_3 over nanosized Cu/SAPO-34 catalysts. *ChemCatChem* **2019**, *11*, 3865-70. DOI
11. Djerad, S.; Tifouti, L.; Crocoll, M.; Weisweiler, W. Effect of vanadia and tungsten loadings on the physical and chemical characteristics of V_2O_5-WO_3/TiO_2 catalysts. *J. Mol. Catal. A. Chem.* **2004**, *208*, 257-65. DOI
12. Martín, J. A.; Yates, M.; Ávila, P.; Suárez, S.; Blanco, J. Nitrous oxide formation in low temperature selective catalytic reduction of nitrogen oxides with V_2O_5/TiO_2 catalysts. *Appl. Catal. B. Environ.* **2007**, *70*, 330-4. DOI
13. Topsøe, N. Y. Mechanism of the selective catalytic reduction of nitric oxide by ammonia elucidated by in situ on-line fourier

transform infrared spectroscopy. *Science* **1994**, *265*, 1217-9. DOI PubMed

14. Li, J.; Chang, H.; Ma, L.; Hao, J.; Yang, R. T. Low-temperature selective catalytic reduction of NO_x with NH_3 over metal oxide and zeolite catalysts - a review. *Catal. Today.* **2011**, *175*, 147-56. DOI
15. Chen, J.; Huang, W.; Bao, S.; et al. A review on the characterization of metal active sites over Cu-based and Fe-based zeolites for NH_3-SCR. *RSC. Adv.* **2022**, *12*, 27746-65. DOI PubMed PMC
16. Wang, Y.; Li, J.; Liu, Z. Selective catalytic reduction of NO_x by NH_3 over Cu-AEI zeolite catalyst: current status and future perspectives. *Appl. Catal. B. Environ.* **2024**, *343*, 123479. DOI
17. Guo, R. T.; Qin, B.; Wei, L. G.; Yin, T. Y.; Zhou, J.; Pan, W. G. Recent progress of low-temperature selective catalytic reduction of NO_x with NH_3 over manganese oxide-based catalysts. *Phys. Chem. Chem. Phys.* **2022**, *24*, 6363-82. DOI PubMed
18. Gao, F.; Tang, X.; Yi, H.; et al. Promotional mechanisms of activity and SO_2 tolerance of Co- or Ni-doped MnOx-CeO_2 catalysts for SCR of NOx with NH_3 at low temperature. *Chem. Eng. J.* **2017**, *317*, 20-31. DOI
19. Gao, F.; Tang, X.; Yi, H.; Zhao, S.; Wang, J.; Gu, T. Improvement of activity, selectivity and H_2O&SO_2-tolerance of micro-mesoporous $CrMn_2O_4$ spinel catalyst for low-temperature NH_3-SCR of NOx. *Appl. Surf. Sci.* **2019**, *466*, 411-24. DOI
20. Li, Y.; Yu, J. Emerging applications of zeolites in catalysis, separation and host–guest assembly. *Nat. Rev. Mater.* **2021**, *6*, 1156-74. DOI
21. Li, Y.; Li, L.; Yu, J. Applications of zeolites in sustainable chemistry. *Chem* **2017**, *3*, 928-49. DOI
22. Kerstens, D.; Smeyers, B.; Van, W. J.; Zhang, Q.; Yu, J.; Sels, B. F. State of the art and perspectives of hierarchical zeolites: practical overview of synthesis methods and use in catalysis. *Adv. Mater.* **2020**, *32*, e2004690. DOI PubMed
23. Sun, Q.; Wang, N.; Yu, J. Advances in catalytic applications of zeolite-supported metal catalysts. *Adv. Mater.* **2021**, *33*, e2104442. DOI PubMed
24. Sun, Q.; Xie, Z.; Yu, J. The state-of-the-art synthetic strategies for SAPO-34 zeolite catalysts in methanol-to-olefin conversion. *Natl. Sci. Rev.* **2018**, *5*, 542-58. DOI
25. Liu, L.; Corma, A. Confining isolated atoms and clusters in crystalline porous materials for catalysis. *Nat. Rev. Mater.* **2021**, *6*, 244-63. DOI
26. Iwamoto, M.; Furukawa, H.; Mine, Y.; Uemura, F.; Mikuriya, S.; Kagawa, S. Copper(II) ion-exchanged ZSM-5 zeolites as highly active catalysts for direct and continuous decomposition of nitrogen monoxide. *J. Chem. Soc. Chem. Commun.* **1986**, 1272-3. DOI
27. Ochońska, J.; Mcclymont, D.; Jodłowski, P.; et al. Copper exchanged ultrastable zeolite Y - A catalyst for NH_3-SCR of NO_x from stationary biogas engines. *Catal. Today.* **2012**, *191*, 6-11. DOI
28. Sullivan, J. A.; Cunningham, J.; Morris, M.; Keneavey, K. Conditions in which Cu-ZSM-5 outperforms supported vanadia catalysts in SCR of NO_x by NH_3. *Appl. Catal. B. Environ.* **1995**, *7*, 137-51. DOI
29. Sjövall, H.; Blint, R. J.; Olsson, L. Detailed kinetic modeling of NH_3 SCR over Cu-ZSM-5. *Appl. Catal. B. Environ.* **2009**, *92*, 138-53. DOI
30. Chen, H.; Sachtler, W. M. Activity and durability of Fe/ZSM-5 catalysts for lean burn NO_x reduction in the presence of water vapor. *Catal. Today.* **1998**, *42*, 73-83. DOI
31. Shi, X.; Liu, F.; Xie, L.; Shan, W.; He, H. NH_3-SCR performance of fresh and hydrothermally aged Fe-ZSM-5 in standard and fast selective catalytic reduction reactions. *Environ. Sci. Technol.* **2013**, *47*, 3293-8. DOI PubMed
32. De-La-Torre, U.; Pereda-Ayo, B.; Moliner, M.; González-Velasco, J. R.; Corma, A. Cu-zeolite catalysts for NO_x removal by selective catalytic reduction with NH_3 and coupled to NO storage/reduction monolith in diesel engine exhaust aftertreatment systems. *Appl. Catal. B. Environ.* **2016**, *187*, 419-27. DOI
33. Xin, Y.; Li, Q.; Zhang, Z. Zeolitic materials for $DeNO_x$ selective catalytic reduction. *ChemCatChem* **2018**, *10*, 29-41. DOI
34. Andana, T.; Rappé, K. G.; Gao, F.; Szanyi, J.; Pereira-hernandez, X.; Wang, Y. Recent advances in hybrid metal oxide–zeolite catalysts for low-temperature selective catalytic reduction of NOx by ammonia. *Appl. Catal. B. Environ.* **2021**, *291*, 120054. DOI
35. Peden, C. H. Cu/Chabazite catalysts for 'Lean-Burn' vehicle emission control. *J. Catal.* **2019**, *373*, 384-9. DOI
36. Lezcano-Gonzaleza, I.; Deka, U.; van, B. H. E.; et al. Chemical deactivation of Cu-SSZ-13 ammonia selective catalytic reduction (NH_3-SCR) systems. *Appl. Catal. B.* **2014**, *154-5*, 339-49. DOI
37. Deka, U.; Lezcano-Gonzalez, I.; Weckhuysen, B. M.; Beale, A. M. Local environment and nature of Cu active sites in zeolite-based catalysts for the selective catalytic reduction of NO_x. *ACS. Catal.* **2013**, *3*, 413-27. DOI
38. Wilken, N.; Wijayanti, K.; Kamasamudram, K.; et al. Mechanistic investigation of hydrothermal aging of Cu-Beta for ammonia SCR. *Appl. Catal. B. Environ.2012*, 111-2:58. DOI
39. Frey, A. M.; Mert, S.; Due-Hansen, J.; Fehrmann, R.; Christensen, C. H. Fe-BEA zeolite catalysts for NH_3-SCR of NO_x. *Catal. Lett.* **2009**, *130*, 1-8. DOI
40. Rahkamaa-tolonen, K.; Maunula, T.; Lomma, M.; Huuhtanen, M.; Keiski, R. L. The effect of NO_2 on the activity of fresh and aged zeolite catalysts in the NH_3-SCR reaction. *Catal. Today.* **2005**, *100*, 217-22. DOI
41. Kwak, J. H.; Tonkyn, R. G.; Kim, D. H.; Szanyi, J.; Peden, C. H. Excellent activity and selectivity of Cu-SSZ-13 in the selective catalytic reduction of NO_x with NH_3. *J. Catal.* **2010**, *275*, 187-90. DOI
42. Kwak, J. H.; Tran, D.; Burton, S. D.; Szanyi, J.; Lee, J. H.; Peden, C. H. Effects of hydrothermal aging on NH_3-SCR reaction over Cu/zeolites. *J. Catal.* **2012**, *287*, 203-9. DOI
43. Wang, Y.; Han, J.; Chen, M.; et al. Low-silica Cu-CHA zeolite enriched with Al pairs transcribed from silicoaluminophosphate seed: synthesis and ammonia selective catalytic reduction performance. *Angew. Chem. Int. Ed. Engl.* **2023**, *62*, e202306174. DOI PubMed

44. Ryu, T.; Ahn, N. H.; Seo, S.; et al. Fully copper-exchanged high-silica LTA zeolites as unrivaled hydrothermally stable NH_3-SCR catalysts. *Angew. Chem. Int. Ed. Engl.* **2017**, *56*, 3256-60. DOI PubMed
45. Jo, D.; Park, G. T.; Ryu, T.; Hong, S. B. Economical synthesis of high-silica LTA zeolites: a step forward in developing a new commercial NH_3-SCR catalyst. *Appl. Catal. B. Environ.* **2019**, *243*, 212-9. DOI
46. Jo, D.; Ryu, T.; Park, G. T.; et al. Synthesis of high-silica LTA and UFI zeolites and NH_3-SCR performance of their copper-exchanged form. *ACS. Catal.* **2016**, *6*, 2443-7. DOI
47. Kim, J.; Cho, S. J.; Kim, D. H. Facile synthesis of KFI-type zeolite and its application to selective catalytic reduction of NO_x with NH_3. *ACS. Catal.* **2017**, *7*, 6070-81. DOI
48. Han, S.; Tang, X.; Wang, L.; et al. Potassium-directed sustainable synthesis of new high silica small-pore zeolite with KFI structure (ZJM-7) as an efficient catalyst for NH_3-SCR reaction. *Appl. Catal. B. Environ.* **2021**, *281*, 119480. DOI
49. Zhu, N.; Shan, Y.; Shan, W.; et al. Distinct NO_2 effects on Cu-SSZ-13 and Cu-SSZ-39 in the selective catalytic reduction of NO_x with NH_3. *Environ. Sci. Technol.* **2020**, *54*, 15499-506. DOI
50. Moliner, M.; Franch, C.; Palomares, E.; Grill, M.; Corma, A. Cu-SSZ-39, an active and hydrothermally stable catalyst for the selective catalytic reduction of NOx. *Chem. Commun.* **2012**, *48*, 8264-6. DOI PubMed
51. Ming, S.; Chen, Z.; Fan, C.; et al. The effect of copper loading and silicon content on catalytic activity and hydrothermal stability of Cu-SAPO-18 catalyst for NH_3-SCR. *Appl. Catal. A. Gen.* **2018**, *559*, 47-56. DOI
52. Fickel, D. W.; D'addio, E.; Lauterbach, J. A.; Lobo, R. F. The ammonia selective catalytic reduction activity of copper-exchanged small-pore zeolites. *Appl. Catal. B. Environ.* **2011**, *102*, 441-8. DOI
53. Godiksen, A.; Stappen, F. N.; Vennestrøm, P. N. R.; et al. Coordination environment of copper sites in Cu-CHA zeolite investigated by electron paramagnetic resonance. *J. Phys. Chem. C.* **2014**, *118*, 23126-38. DOI
54. Chen, D.; Khetan, A.; Lei, H.; et al. Copper site motion promotes catalytic NO_x reduction under zeolite confinement. *Environ. Sci. Technol.* **2023**, *57*, 16121-30. DOI PubMed
55. Paolucci, C.; Khurana, I.; Parekh, A. A.; et al. Dynamic multinuclear sites formed by mobilized copper ions in NO_x selective catalytic reduction. *Science* **2017**, *357*, 898-903. DOI PubMed
56. Paolucci, C.; Parekh, A. A.; Khurana, I.; et al. Catalysis in a cage: condition-dependent speciation and dynamics of exchanged Cu cations in SSZ-13 zeolites. *J. Am. Chem. Soc.* **2016**, *138*, 6028-48. DOI
57. Kim, Y. J.; Lee, J. K.; Min, K. M.; Hong, S. B.; Nam, I.; Cho, B. K. Hydrothermal stability of CuSSZ13 for reducing NOx by NH_3. *J. Catal.* **2014**, *311*, 447-57. DOI
58. Han, S.; Ye, Q.; Cheng, S.; Kang, T.; Dai, H. Effect of the hydrothermal aging temperature and Cu/Al ratio on the hydrothermal stability of CuSSZ-13 catalysts for NH_3-SCR. *Catal. Sci. Technol.* **2017**, *7*, 703-17. DOI
59. Song, J.; Wang, Y.; Walter, E. D.; et al. Toward rational design of Cu/SSZ-13 selective catalytic reduction catalysts: implications from atomic-level understanding of hydrothermal stability. *ACS. Catal.* **2017**, *7*, 8214-27. DOI
60. Iorio JR, Gounder R. Controlling the isolation and pairing of aluminum in chabazite zeolites using mixtures of organic and inorganic structure-directing agents. *Chem. Mater.* **2016**, *28*, 2236-47. DOI
61. Iorio JR, Nimlos CT, Gounder R. Introducing catalytic diversity into single-site chabazite zeolites of fixed composition via synthetic control of active site proximity. *ACS. Catal.* **2017**, *7*, 6663-74. DOI
62. Zhang, J.; Shan, Y.; Zhang, L.; et al. Importance of controllable Al sites in CHA framework by crystallization pathways for NH_3-SCR reaction. *Appl. Catal. B. Environ.* **2020**, *277*, 119193. DOI
63. Gao, F.; Wang, Y.; Washton, N. M.; Kollár, M.; Szanyi, J.; Peden, C. H. F. Effects of alkali and alkaline earth cocations on the activity and hydrothermal stability of Cu/SSZ-13 NH_3-SCR catalysts. *ACS. Catal.* **2015**, *5*, 6780-91. DOI
64. Usui, T.; Liu, Z.; Ibe, S.; et al. Improve the hydrothermal stability of Cu-SSZ-13 zeolite catalyst by loading a small amount of Ce. *ACS. Catal.* **2018**, *8*, 9165-73. DOI
65. Chen, M.; Li, J.; Xue, W.; et al. Unveiling secondary-ion-promoted catalytic properties of Cu-SSZ-13 zeolites for selective catalytic reduction of NO_x. *J. Am. Chem. Soc.* **2022**, *144*, 12816-24. DOI PubMed
66. Chen, M.; Zhao, W.; Wei, Y.; et al. La ions-enhanced NH_3-SCR performance over Cu-SSZ-13 catalysts. *Nano. Res.* **2023**, *16*, 12126-33. DOI
67. Kang, N.; Wang, Y.; Wen, C. Z.; et al. Understanding enhancement of strong Copper-Yttrium interactions on catalytic properties of Cu/Y-SSZ-13 for NH_3-SCR. *Chem. Eng. J.* **2023**, *475*, 146114. DOI
68. Iwasaki, M.; Shinjoh, H. A comparative study of "standard", "fast" and "NO_2" SCR reactions over Fe/zeolite catalyst. *Appl. Catal. A. Gen.* **2010**, *390*, 71-7. DOI
69. Colombo, M.; Nova, I.; Tronconi, E. A comparative study of the NH_3-SCR reactions over a Cu-zeolite and a Fe-zeolite catalyst. *Catal. Today.* **2010**, *151*, 223-30. DOI
70. Colombo, M.; Nova, I.; Tronconi, E. Detailed kinetic modeling of the NH_3–NO/NO_2 SCR reactions over a commercial Cu-zeolite catalyst for Diesel exhausts after treatment. *Catal. Today.* **2012**, *197*, 243-55. DOI
71. Bendrich, M.; Scheuer, A.; Hayes, R.; Votsmeier, M. Unified mechanistic model for Standard SCR, Fast SCR, and NO_2 SCR over a copper chabazite catalyst. *Appl. Catal. B. Environ.* **2018**, *222*, 76-87. DOI
72. Grossale, A.; Nova, I.; Tronconi, E.; Chatterjee, D.; Weibel, M. The chemistry of the NO/NO_2–NH_3 "fast" SCR reaction over Fe-ZSM5 investigated by transient reaction analysis. *J. Catal.* **2008**, *256*, 312-22. DOI
73. Janssens, T. V. W.; Falsig, H.; Lundegaard, L. F.; et al. A consistent reaction scheme for the selective catalytic reduction of nitrogen

oxides with ammonia. *ACS. Catal.* **2015**, *5*, 2832-45. DOI

74. Schuler, A.; Votsmeier, M.; Kiwic, P.; et al. NH_3-SCR on Fe zeolite catalysts - from model setup to NH_3 dosing. *Chem. Eng. J.* **2009**, *154*, 333-40. DOI
75. Chen, H.; Wei, Z.; Kollar, M.; et al. A comparative study of N_2O formation during the selective catalytic reduction of NOx with NH_3 on zeolite supported Cu catalysts. *J. Catal.* **2015**, *329*, 490-8. DOI
76. Shi, X.; Liu, F.; Shan, W.; He, H. Hydrothermal deactivation of Fe-ZSM-5 prepared by different methods for the selective catalytic reduction of NO_x with NH_3. *Chin. J. Catal.* **2012**, *33*, 454-64. DOI
77. Yin, C.; Cheng, P.; Li, X.; Yang, R. T. Selective catalytic reduction of nitric oxide with ammonia over high-activity Fe/SSZ-13 and Fe/one-pot-synthesized Cu-SSZ-13 catalysts. *Catal. Sci. Technol.* **2016**, *6*, 7561-8. DOI
78. Wang, Y.; Xie, L.; Liu, F.; Ruan, W. Effect of preparation methods on the performance of CuFe-SSZ-13 catalysts for selective catalytic reduction of NO_x with NH_3. *J. Environ. Sci.* **2019**, *81*, 195-204. DOI PubMed
79. Wan, J.; Chen, J.; Zhao, R.; Zhou, R. One-pot synthesis of Fe/Cu-SSZ-13 catalyst and its highly efficient performance for the selective catalytic reduction of nitrogen oxide with ammonia. *J. Environ. Sci.* **2021**, *100*, 306-16. DOI PubMed
80. Jouini, H.; Mejri, I.; Petitto, C.; et al. Characterization and NH_3-SCR reactivity of Cu-Fe-ZSM-5 catalysts prepared by solid state ion exchange: the metal exchange order effect. *Micropor. Mesopor. Mat.* **2018**, *260*, 217-26. DOI
81. Sultana, A.; Sasaki, M.; Suzuki, K.; Hamada, H. Tuning the NOx conversion of Cu-Fe/ZSM-5 catalyst in NH_3-SCR. *Catal. Commun.* **2013**, *41*, 21-5. DOI
82. Ren, L.; Zhu, L.; Yang, C.; et al. Designed copper-amine complex as an efficient template for one-pot synthesis of Cu-SSZ-13 zeolite with excellent activity for selective catalytic reduction of NOx by NH_3. *Chem. Commun.* **2011**, *47*, 9789-91. DOI
83. Xie, L.; Liu, F.; Shi, X.; Xiao, F.; He, H. Effects of post-treatment method and Na co-cation on the hydrothermal stability of Cu-SSZ-13 catalyst for the selective catalytic reduction of NO with NH_3. *Appl. Catal. B. Environ.* **2015**, *179*, 206-12. DOI
84. Xie, L.; Liu, F.; Ren, L.; Shi, X.; Xiao, F. S.; He, H. Excellent performance of one-pot synthesized Cu-SSZ-13 catalyst for the selective catalytic reduction of NOx with NH_3. *Environ. Sci. Technol.* **2014**, *48*, 566-72. DOI PubMed
85. Shan, Y.; Du, J.; Yu, Y.; Shan, W.; Shi, X.; He, H. Precise control of post-treatment significantly increases hydrothermal stability of in-situ synthesized cu-zeolites for NH_3-SCR reaction. *Appl. Catal. B. Environ.* **2020**, *266*, 118655. DOI
86. Zhang, T.; Li, J.; Liu, J.; et al. High activity and wide temperature window of Fe-Cu-SSZ-13 in the selective catalytic reduction of NO with ammonia. *AIChE. J.* **2015**, *61*, 3825-37. DOI
87. Xu, R.; Wang, Z.; Liu, N.; Dai, C.; Zhang, J.; Chen, B. Understanding Zn Functions on hydrothermal stability in a one-pot-synthesized Cu&Zn-SSZ-13 catalyst for NH_3 selective catalytic reduction. *ACS. Catal.* **2020**, *10*, 6197-212. DOI
88. Zhou, X.; Chen, Z.; Guo, Z.; et al. One-pot hydrothermal synthesis of dual metal incorporated CuCe-SAPO-34 zeolite for enhancing ammonia selective catalytic reduction. *J. Hazard. Mater.* **2021**, *405*, 124177. DOI PubMed
89. Du, J.; Wang, J.; Shi, X.; Shan, Y.; Zhang, Y.; He, H. Promoting effect of Mn on in situ synthesized Cu-SSZ-13 for NH_3-SCR. *Catalysts* **2020**, *10*, 1375. DOI
90. Chen, Z.; Liu, Q.; Guo, L.; et al. The promoting mechanism of in situ Zr doping on the hydrothermal stability of Fe-SSZ-13 catalyst for NH_3-SCR reaction. *Appl. Catal. B. Environ.* **2021**, *286*, 119816. DOI
91. Pang, L.; Fan, C.; Shao, L.; et al. The Ce doping Cu/ZSM-5 as a new superior catalyst to remove NO from diesel engine exhaust. *Chem. Eng. J.* **2014**, *253*, 394-401. DOI
92. Wang, J.; Liu, J.; Tang, X.; Xing, C.; Jin, T. The promotion effect of niobium on the low-temperature activity of Al-rich Cu-SSZ-13 for selective catalytic reduction of NO_x with NH_3. *Chem. Eng. J.* **2021**, *418*, 129433. DOI
93. Zhu, N.; Hou, L.; Li, S.; Deng, Y. Understanding Na functions on distribution of Cu species within Cu-SSZ-13 for the selective reduction of NO_x with NH_3. *Sep. Purif. Technol.* **2024**, *347*, 127630. DOI
94. Lv, W.; Wang, S.; Wang, P.; et al. Regulation of Al distributions and Cu^{2+} locations in SSZ-13 zeolites for NH_3-SCR of NO by different alkali metal cations. *J. Catal.* **2021**, *393*, 190-201. DOI
95. Lee, H.; Song, I.; Jeon, S. W.; Kim, D. H. Control of the Cu ion species in Cu-SSZ-13 *via* the introduction of Co^{2+} co-cations to improve the NH_3-SCR activity. *Catal. Sci. Technol.* **2021**, *11*, 4838-48. DOI
96. U.S. Drive. Advanced combustion and emission control technical team roadmap. 2013. Available from: https://www1.eere.energy.gov/vehiclesandfuels/pdfs/program/acec_roadmap_june2013.pdf. [Last accessed on 5 Aug 2024].
97. Zhang, T.; Qiu, F.; Li, J. Design and synthesis of core-shell structured *meso*-Cu-SSZ-13@mesoporous aluminosilicate catalyst for SCR of NO_x with NH_3: enhancement of activity, hydrothermal stability and propene poisoning resistance. *Appl. Catal. B. Environ.* **2016**, *195*, 48-58. DOI
98. Shih, A. J.; González, J. M.; Khurana, I.; et al. Influence of ZCuOH, Z_2Cu, and extraframework Cu_xOy species in Cu-SSZ-13 on N_2O formation during the selective catalytic reduction of NO_x with NH_3. *ACS. Catal.* **2021**, *11*, 10362-76. DOI
99. Zhang, Y.; Zhu, H.; Zhang, T.; et al. Revealing the synergistic deactivation mechanism of hydrothermal aging and SO_2 poisoning on Cu/SSZ-13 under SCR condition. *Environ. Sci. Technol.* **2022**, *56*, 1917-26. DOI
100. Ye, X.; Schmidt, J. E.; Wang, R. P.; et al. Deactivation of Cu-exchanged automotive-emission NH_3-SCR catalysts elucidated with nanoscale resolution using scanning transmission X-ray microscopy. *Angew. Chem. Int. Ed. Engl.* **2020**, *59*, 15610-7. DOI PubMed PMC
101. Cui, Y.; Wang, Y.; Mei, D.; et al. Revisiting effects of alkali metal and alkaline earth co-cation additives to Cu/SSZ-13 selective catalytic reduction catalysts. *J. Catal.* **2019**, *378*, 363-75. DOI

102. Chen, M.; Zhao, W.; Wei, Y.; et al. Improving the hydrothermal stability of Al-rich Cu-SSZ-13 zeolite *via* Pr-ion modification. *Chem. Sci.* **2024**, *15*, 5548-54. DOI PubMed PMC
103. Clark, A. H.; Nuguid, R. J. G.; Steiger, P.; et al. Selective catalytic reduction of NO with NH_3 on Cu-SSZ-13: deciphering the low and high-temperature rate-limiting steps by transient XAS experiments. *ChemCatChem* **2020**, *12*, 1429-35. DOI
104. Chen, L.; Janssens, T. V. W.; Vennestrøm, P. N. R.; Jansson, J.; Skoglundh, M.; Grönbeck, H. A complete multisite reaction mechanism for low-temperature NH_3-SCR over Cu-CHA. *ACS. Catal.* **2020**, *10*, 5646-56. DOI
105. Liu, C.; Kubota, H.; Toyao, T.; Maeno, Z.; Shimizu, K. Mechanistic insights into the oxidation of copper(I) species during NH_3-SCR over Cu-CHA zeolites: a DFT study. *Catal. Sci. Technol.* **2020**, *10*, 3586-93. DOI
106. Feng, Y.; Wang, X.; Janssens, T. V. W.; et al. First-principles microkinetic model for low-temperature NH_3-assisted selective catalytic reduction of NO over Cu-CHA. *ACS. Catal.* **2021**, *11*, 14395-407. DOI
107. Hu, W.; Selleri, T.; Gramigni, F.; et al. On the redox mechanism of low-temperature NH_3-SCR over Cu-CHA: a combined experimental and theoretical study of the reduction half cycle. *Angew. Chem. Int. Ed. Engl.* **2021**, *60*, 7197-204. DOI PubMed
108. Feng, Y.; Janssens, T. V. W.; Vennestrøm, P. N. R.; Jansson, J.; Skoglundh, M.; Grönbeck, H. The role of H^+- and Cu^+-sites for N_2O formation during NH_3-SCR over Cu-CHA. *J. Phys. Chem. C.* **2021**, *125*, 4595-601. DOI
109. Chen, Z.; Guo, L.; Qu, H.; Liu, L.; Xie, H.; Zhong, Q. Controllable positions of Cu^{2+} to enhance low-temperature SCR activity on novel Cu-Ce-La-SSZ-13 by a simple one-pot method. *Chem. Commun.* **2020**, *56*, 2360-3. DOI PubMed
110. Yue, Y.; Liu, B.; Qin, P.; et al. One-pot synthesis of FeCu-SSZ-13 zeolite with superior performance in selective catalytic reduction of NO by NH_3 from natural aluminosilicates. *Chem. Eng. J.* **2020**, *398*, 125515. DOI
111. Chen, M.; Wei, Y.; Han, J.; Yan, W.; Yu, J. Enhancing catalytic performance of Cu-SSZ-13 for the NH_3-SCR reaction *via in situ* introduction of Fe^{3+} with diatomite. *Mater. Chem. Front.* **2021**, *5*, 7787-95. DOI
112. Han, J.; Jin, X.; Song, C.; et al. Rapid synthesis and NH_3-SCR activity of SSZ-13 zeolite *via* coal gangue. *Green. Chem.* **2020**, *22*, 219-29. DOI

Mengyang Chen

Mengyang Chen received his B.Sc. degree in chemistry from Guangxi University in 2016 and his Ph.D. in inorganic chemistry from Jilin University in 2022 under the supervision of Prof. Jihong Yu. He then joined the School of Pharmaceutical and Chemical Engineering at Taizhou University. His current research focuses on the synthesis of crystalline porous materials for environmental catalysis.

Shi-Bin Ren

Shi-Bin Ren received his Ph.D. in 2010 and worked as a postdoctoral research fellow in the School of Chemistry and Chemical Engineering, Nanjing University, from 2012 to 2016. He also served as a visiting scholar at the University of Liverpool from 2016 to 2017. Now, he is a professor in the School of Pharmaceutical and Chemical Engineering at Taizhou University. His research specializes in porous materials in photocatalysis, electrocatalysis, photo/electrocatalysis and energy storage.

De-Man Han

De-Man Han received his Ph.D. from Naikai University in 2007. He is currently a full professor in the School of Pharmaceutical and Chemical Engineering at Taizhou University and has published over 100 scientific papers. His research interests primarily involve the development of various optical/electrochemical biosensors and environmental analysis.